FINAL REPORT

MATERIAL RESPONSE STUDIES (MARS I)

Volume III

DEVELOPMENT OF MULTIAXIAL STRESS HIGH STRAIN-RATE TECHNIQUES

by

S J Green
J D Leasia
R D Perkins
C J Maiden

Materials & Structures Laboratory
Manufacturing Development
General Motors Corporation

Technical Report SAMSO TR 68-71-Vol. III
1968, January

Prepared For
Space and Missile Systems Organization
Deputy for Ballistic Missile Reentry Systems
Air Force Systems Command
Norton Air Force Base, California
Contract No. F04694-67-C-0033

SAMSO TR-68-71- Vol. III

Copy No. [redacted]

FINAL REPORT

...ATERIAL RESPONSE STUDIES (MARS I)

Volume III

DEVELOPMENT OF MULTIAXIAL STRESS HIGH STRAIN-RATE TECHNIQUES

by

S. J. Green
J. D. Leasia
R. D. Perkins
C. J. Maiden

Materials & Structures Laboratory
Manufacturing Development
General Motors Corporation

FOREWORD

This report was prepared by the Applied Mechanics Section of the Materials and Structures Laboratory, Manufacturing Development, General Motors Technical Center, Warren, Michigan, under Air Force Contract FO4694-67-C-0033. The work was administered by the Air Force Space and Missile Systems Organization, Air Force Systems Command, with Major N. J. Azzarita as technical administrator. Mr. R. B. Mortensen, Mr. R. A. Needham, Dr. F. A. Field and Dr. W. Barry of the Aerospace Corporation served as principal technical monitors for the Air Force.

Because of the different types of work performed in this study, the report is divided into seven separately bound volumes listed below. The present volume is one of these parts.

Volume I:	Summary
Volume II:	High Strain-Rate Response of Three Heat Shield Materials at Elevated Temperatures
Volume III:	Development of Multiaxial Stress High Strain-Rate Techniques
Volume IV:	Dynamic Mechanical Properties at Ablative Temperatures - Techniques
Volume V:	Dynamic Behavior of Polymers and Composites
Volume VI:	Mechanical Properties of Beryllium at High Strain Rates
Volume VII:	Ablation Test Specimen Environment at High Temperature

The work was performed under the supervision of Dr. C. J. Maiden. Program Manager and Principal Investigator was Mr. S. J. Green. Other project scientists included:

S. G. Babcock, Dr. A. Kumar, R. G. Kumble, J. D. Leasia, W. F. Dais, R. D. Perkins, F. L. Schierloh.

This report is UNCLASSIFIED. This document may be further distributed by any holder only with specific prior approval of Space and Missile Systems Organization ([redacted] Air Force Base, California [redacted]

This technical report has been reviewed and is approved.

Nicholas J. Azzarita
Major, USAF
Project Officer
SAMSO/SMYSE

ABSTRACT

Results reported here are on the development of techniques to determine material yield and/or fracture under multiaxial stress loadings at strain rates to 10^2/second. An evaluation of various methods of biaxial and triaxial loading was made in order to determine a suitable method of testing both structural and ablator materials. Hence, the loading method and tubular specimen configuration are for nonhomogeneous, nonisotropic, brittle materials as well as more conventional ductile metals. A Biaxial Strain-Rate Machine has been built and some preliminary tests conducted. Details of the design and instrumentation are presented as well as preliminary data on an aluminum alloy.

(Page iv is blank)

TABLE OF CONTENTS

	Page
FORWARD	ii
ABSTRACT	iii
INTRODUCTION	1
SECTION I - BIAXIAL AND TRIAXIAL LOADING SYSTEMS	3
SECTION II - SPECIMEN CONFIGURATION	8
SECTION III - MACHINE DESIGN	11
SECTION IV - INSTRUMENTATION	27
SECTION V - PRELIMINARY DATA	31
ACKNOWLEDGMENTS	37
REFERENCES	38
APPENDIX A - SPECIFICATIONS FOR BIAXIAL MACHINE	43
APPENDIX B - ANALYTICAL STUDY OF PISTON MOTION	45
APPENDIX C - DETAILS OF FRAME PRELOAD	57
DD FORM 1473 - DOCUMENT CONTROL DATA - R & D	61

LIST OF ILLUSTRATIONS

Figure	Title	Page
1	Photograph of Biaxial Machine Specimens of Metallic and Composite Materials	10
2	Schematic Diagram of Biaxial Medium Strain-Rate Machine	12
3	Photograph of Biaxial Medium Strain-Rate Machine	13
4	Flow-chart of Parameters Investigated During Piston Motion Study	15
5	Sectional View of 12.5 inch Diameter, Axial Loading Cylinder	16
6	Sectional View of Fast Acting Exhaust Valve	18
7	Hydraulic Diagram for Biaxial Machine Loading Cylinder	20
8	Control Panel for Biaxial Machine	21
9	Sectional View of 6 inch Diameter, Circumferential Loading Cylinder	23
10	Sectional View of Specimen Package for Axial Compression and Circumferential Tension (Metallic Specimen)	24
11	Photograph of a Test Package for Metal Specimens	25
12	Schematic Diagram of Instrumentation for One Transducer on the Biaxial Machine	28
13	Block Diagram of Data Measurement and Reduction for Biaxial Machine	30
14	Stress Versus Strain for 6061-T651 Aluminum	32
15	Photograph of Aluminum Tube Tested under Axial Load Only	33
16	Photograph of Aluminum Tube Tested under Circumferential Load (With Constant Axial Load)	33

Figure	Title	Page
17	Stress and Strain Versus Time for an Extensively Instrumented Alumirum Tube Under Axial Load Only	35
18	Strain Versus Time at Three Positions Along the Axis of an Aluminum Tube Loaded with Internal Pressure (With Constant Axial Load)	36

LIST OF ILLUSTRATIONS IN APPENDIXES

Figure	Title	Page
B-1	Force System for Piston Motion Study	46
B-2	Example of the Effect of Initial Reservoir Pressure on Piston Velocity	53
B-3	Example of the Effect of Damping on Piston Velocity	54
B-4	Predicted Axial Strain on a Quartz Phenolic Tube	55
B-5	Predicted Circumferential Strain on a Quartz Phenolic Tube	56
C-1	Force System for Frame Preload	57
C-2	Force - Deflection Behavior of Tie Rods	58

(Page viii is blank)

INTRODUCTION

Determining material response, i.e. strength, stiffness, ductility, and fracture under rapid loading or impulsive loading conditions, has become a necessity as structural applications are subjected to such loadings. Blast loading of structures from conventional blast or nuclear devices, high energy forming techniques and high velocity impact are present applications requiring dynamic material properties. Strain rates to $10\text{-}10^2$/second are common in blast loading problems and rates to $10^5\text{-}10^8$/second are possible in shock type loads.

Techniques have been developed to investigate material behavior under high strain-rate uniaxial stress loading,[1-6] and high strain-rate data have been generated on a variety of materials.[7-14] Test techniques are difficult, particularly at the highest strain rates, and must be carefully reviewed before accepting published data. Material response under high strain-rate biaxial or triaxial stress loading is even more difficult to obtain, and only a few attempts at obtaining fundamental data have been made.[15-18]

The most reliable multiaxial stress, high strain-rate data on a wide variety of materials is found in recent flat plate work, where experimenters have impacted one plate into another, thereby creating a uniaxial strain loading.[19-24] Strain rates are 10^5/second and higher in the shock front produced upon impact and decrease as the shock front is attenuated. The conventional stress-strain curve cannot be obtained from these tests, but yield (or fracture) at various strain rates can

be studied to some extent by measuring the "elastic" wave magnitude as the shock front is attenuated. These data can be compared to uniaxial stress data by resorting to some assumed yield/fracture criterion. A general yield/fracture criterion, however, cannot be obtained from these tests. The discussion here will not include the flat plate experiments, since only statically determinant loadings are considered.

After searching the available literature on means of creating a statically-determinant biaxial loading, the method of loading a tubular specimen with axial load and internal or external fluid pressure was selected as the most suitable for nonhomogeneous, nonisotropic materials. On this basis a machine capable of producing these loadings for strain rates to 10^2/second was designed and constructed.

SECTION I

BIAXIAL AND TRIAXIAL LOADING SYSTEMS

To date, multiaxial high strain-rate loading systems have been limited to homogeneous, isotropic (or at least nearly isotropic) materials of low or moderate strength and reasonable ductility, namely, poly-crystalline metals such as aluminum (or aluminum alloys) and soft steels. The following review of the techniques used on these materials was used to determine the system most adaptable to the more difficult materials.

Lindholm and Yeakley have used a small tubular specimen simultaneously subjected to tension and torsion at strain rates to 10-30/second.[15] During the test, the directions of principal stresses and strains are not fixed, but rotate as the specimen is loaded. Although this technique works well for ductile metals, instrumentation and interpretation of data would be difficult for brittle, anisotropic materials. Furthermore, the small specimen used would impose difficulties for nonhomogeneous materials, such as ablative composites.

Gerard and Papirno used a thin membrane specimen placed over a large diameter cylinder and loaded by an air blast.[16] Their results are for strain rates to 1-4/second on ductile metals. This method produces only equal biaxial tension, and would impose serious limitations on the interpretation of the data for nonhomogeneous, brittle materials.

Hoge used small hollow cylindrical test specimens with part of the axial load (produced from dynamic internal fluid pressure) carried by an external rod.[17] By varying the amount of axial load carried by the rod, which can be done by changing specimen geometry, different ratios of axial to circumferential loads can be achieved. The method is clever, but suffers from end effects which propagate into the gage section, and is restricted to proportional load, tension-tension, type tests only.

Chalupnik and Ripperger[18] performed experiments using the split Hopkinson bar technique[2] under constant hydrostatic pressure. This method is particularly attractive when the yield and/or fracture is governed by hydrostatic pressure, and offers less favor for materials little affected by hydrostatic pressure.

A number of articles appear in the literature for biaxial or triaxial "quasistatic" methods. Work by Davis[25] on thin walled tubes subjected to tension and internal pressure is typical, and presents classical work on static behavior of metals. Others[26-32] have done similar work on metals using thin walled tubes subjected to tension and internal pressure or torsion. Cornet and Grassi,[33] Ely,[34] and Babal and Sines[35] have performed static experiments on thin walled tubes of brittle materials under axial tension or compression and internal pressure. This system is readily adaptable to the nonhomogeous materials and was selected as the best method for multiaxial studies on various materials. Before proceeding with detailed discussion of the tubular specimen technique, several other methods of biaxial or triaxial loading will be reviewed.

Biaxial stress tests were performed by Nadai[36] and by Wahl, et.al.,[37] using a spinning disc. The results and techniques are elegant and afford a relatively simple method of producing high loads. Quick spin-ups could produce high strain rates; however, even with thin walled discs, the stress distribution would be difficult to specify.

Flat plates under uniform tension in two directions have been used by Johnson[38] and Shiratori and Ikagami.[39] This is probably the simplest biaxial test to visualize, but is restricted to tension-tension tests. Furthermore, elimination of end effects is difficult for small strains and virtually impossible for larger deformations.

Manjoine[40] suggested a notched specimen, whereby biaxial stresses are produced at the base of the notch. This technique, which could be performed at low and intermediate strain rates for investigations of the fracture of brittle materials, may be useful in conjunction with more general loadings. The notched specimen technique, however, would be restricted to brittle homogeneous materials.

The most classical triaxial test is loading under hydrostatic pressure. Bridgman's extensive work[41] and that of Pugh[42] present results on a variety of materials. Tests under hydrostatic pressure are routinely performed on geological materials[43,44] where yield/fracture is very much a function of pressure. A rig is being designed by Logan[45] to conduct dynamic axial load tests under static pressure on geological materials following the driving unit design of Maiden and Green.[10] This type of test, i.e. dynamic axial load under static hydrostatic pressure, is attractive for studying the

fracture of composites and other ablative materials. The study could easily include the very high stain rates using the technique of Chalupnik and Ripperger.[19]

Of the various specimen configurations and loading methods reviewed, the thin walled tube subjected to axial tension or compression and internal or external pressure is the most adaptable to a wide variety of materials. Many materials can be either machined or fabricated directly into a tubular shape. The loading of this configuration allows tests in all quadrants of principal stress space, i.e. tension-tension, compression-compression, tension-compression, compression-tension, and the directions of principal stresses are known and fixed during the test.

Strain rates approaching those where stress waves can no longer be averaged are readily attainable; on the order of $10\text{-}10^2$/second for most materials. Higher rates, where stress gradients exist in the specimen gage section must be avoided because of uncertainties in the data interpretation. Multiaxial stress tests at higher strain rates, in the region of $10^2\text{-}10^4$/second, are apt to yield only quantitative results, at best, for any specimen configuration. Applying the same techniques as for the split Hopkinson bar[2] cannot be done because end effects produced by the biaxial loading of any configuration will require "large" specimens, thereby violating the requirements of the technique.[6] Uniaxial strain, flat plate, experiments may be conducted for multiaxial loading for strain rates of 10^4/second and greater as long as the gage section of the specimen (target) is sufficiently large

that side reflections do not enter until the test is completed.[20] However, this technique is readily adaptable only to statically indeterminate uniaxial strain. Because of these complications, this multiaxial loading study was restricted to rates up to $10\text{-}10^2$/second.

SECTION II

SPECIMEN CONFIGURATION

Suitable dimensions for a biaxially loaded tubular specimen of a nonhomogenous, nonisotropic composite material were determined based upon previously obtained uniaxial stress data[46]. The prime consideration was the need for specimens which would represent the bulk properties of the material. Therefore, from information concerning the behavior of typical ablator composites as a function of specimen size,[46] a minimum wall thickness of 0.250 inch was determined. Although the wall thickness could be made larger without impairing the data, significantly smaller thicknesses would result in data influenced by the specimen size.

Once the wall thickness was determined, the outside diameter was fixed based on as large as possible outside diameter to wall thickness ratio (D/t) with reasonable cross-sectional area. This portion of the specimen design was coupled closely with the loading piston design study discussed in Section III. Briefly, calculating the piston dynamics with a specimen size as an initial condition, it was determined that specimens with a wall thickness of 0.250 inch and a (D/t) ratio greater than 10 would require driving systems incompatible with the design criteria of the basic machine; in particular a quick acceleration to a rate of 10/second on a high strength composite material such as quartz phenolic.

Having fixed the wall thickness and outside diameter, the only remaining parameter was specimen length. This parameter

was influenced by maximum machine dimensions (dictated by limits placed on the elastic deformation of the machine during a test), maximum rate considerations, and a requirement, based on previous uniaxial stress work, of having a minimum unsupported specimen length-to-diameter (ℓ/D) ratio of 1.33. The final over all length was determined to be 6.0 inch with 5.0 inch of unsupported length.

Although the specimen was designed about a composite material, aluminum alloy was considered the best material for initial testing because of its medium strength, good ductility, and ease of fabrication. Therefore, an aluminum specimen was designed using smaller wall thickness (0.125 inch) for a higher (D/t) and a shorter length for a smaller (ℓ/D) ratio made possible by the homogeneity of the material. Photographs of the aluminum and composite (in this case Micarta) specimens are shown in Figure 1.

Specimens for testing under axial tension are being designed. For the composite materials, the difficult task of assessing the efficiency of various mechanical interlocking arrangements, compatible with specimen fabrication, is in progress. For metallic materials, long specimens, with relatively small diameters and thin walls are being designed along with suitable mechanical gripping techniques. The tubular metallic specimens for axial tension may be considerably smaller in diameter and longer in length because of the elimination of buckling associated with the compressive axial loadings.

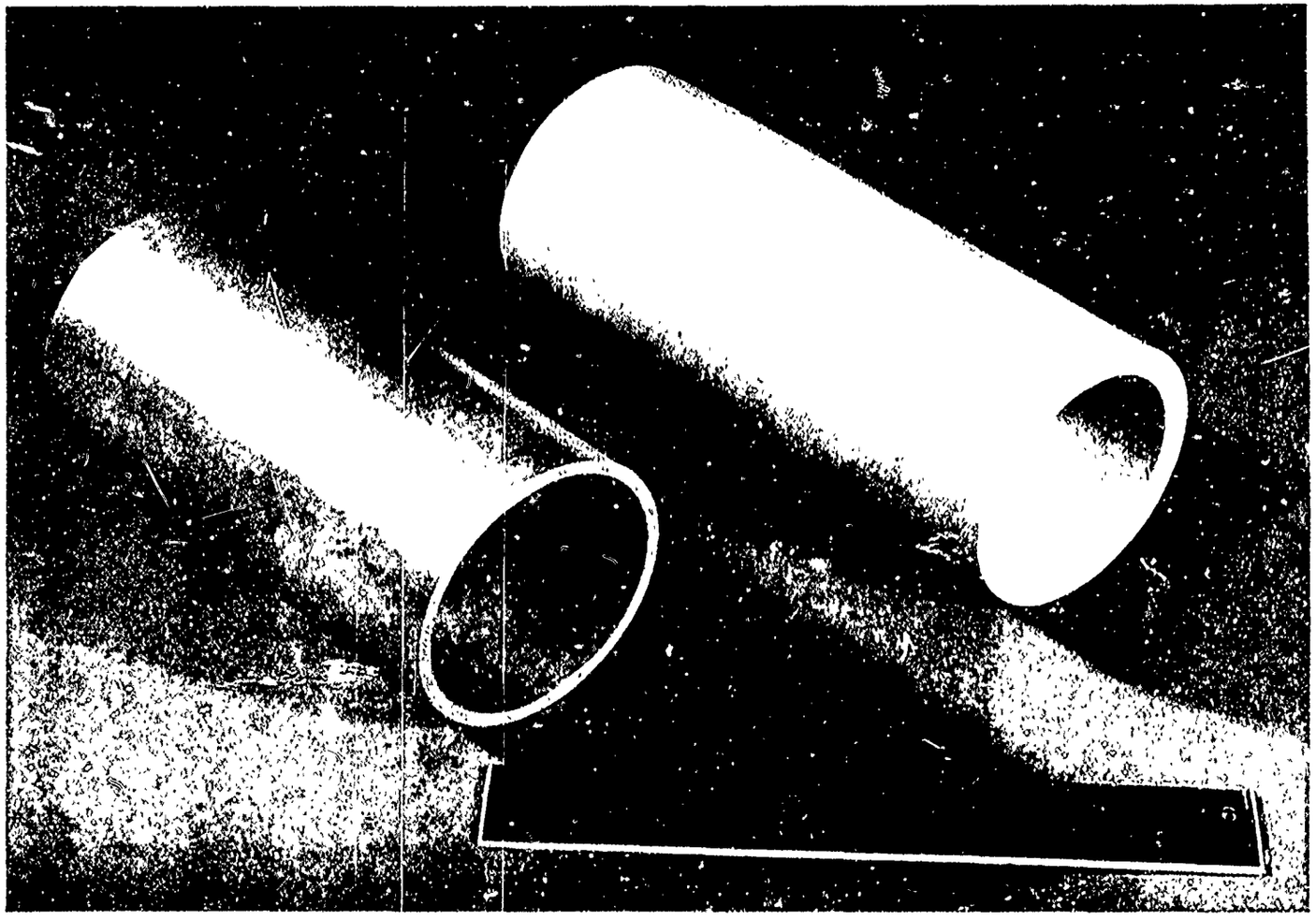

Figure 1 Photograph of Biaxial Machine Specimens of Metallic and Composite Materials

SECTION III

MACHINE DESIGN

The machine described here (shown in Figures 2 and 3) develops a biaxial state of stress by applying an axial load and a circumferential load (by fluid pressure) on a tubular specimen through two independent gas-operated cylinders. A 12.5 inch bore cylinder is used to provide the axial load to the specimen while a 6 inch bore cylinder is used to load an auxiliary piston which, in turn, pressurizes a fluid for circumferential loading of the specimen. The specimen is pressurized internally for circumferential tension, and externally for circumferential compression.

The machine is operated by charging each cylinder with gas, which may be air, nitrogen, or helium, introduced at equal pressure into a large reservoir in back of the piston, and into a small reservoir in front of the piston. The piston moves forward when the small reservoir is exhausted by flow through an orifice.

Exhaust of the small reservoir is initiated through the opening of a fast acting valve mounted downstream of the orifice. Piston velocity, and hence the rate of loading, is controlled by the type and pressure of the working gas, the orifice size, and, to some extent, the specimen. In addition, a variable hydraulic damper is attached to each piston to damp undesirable piston oscillations.

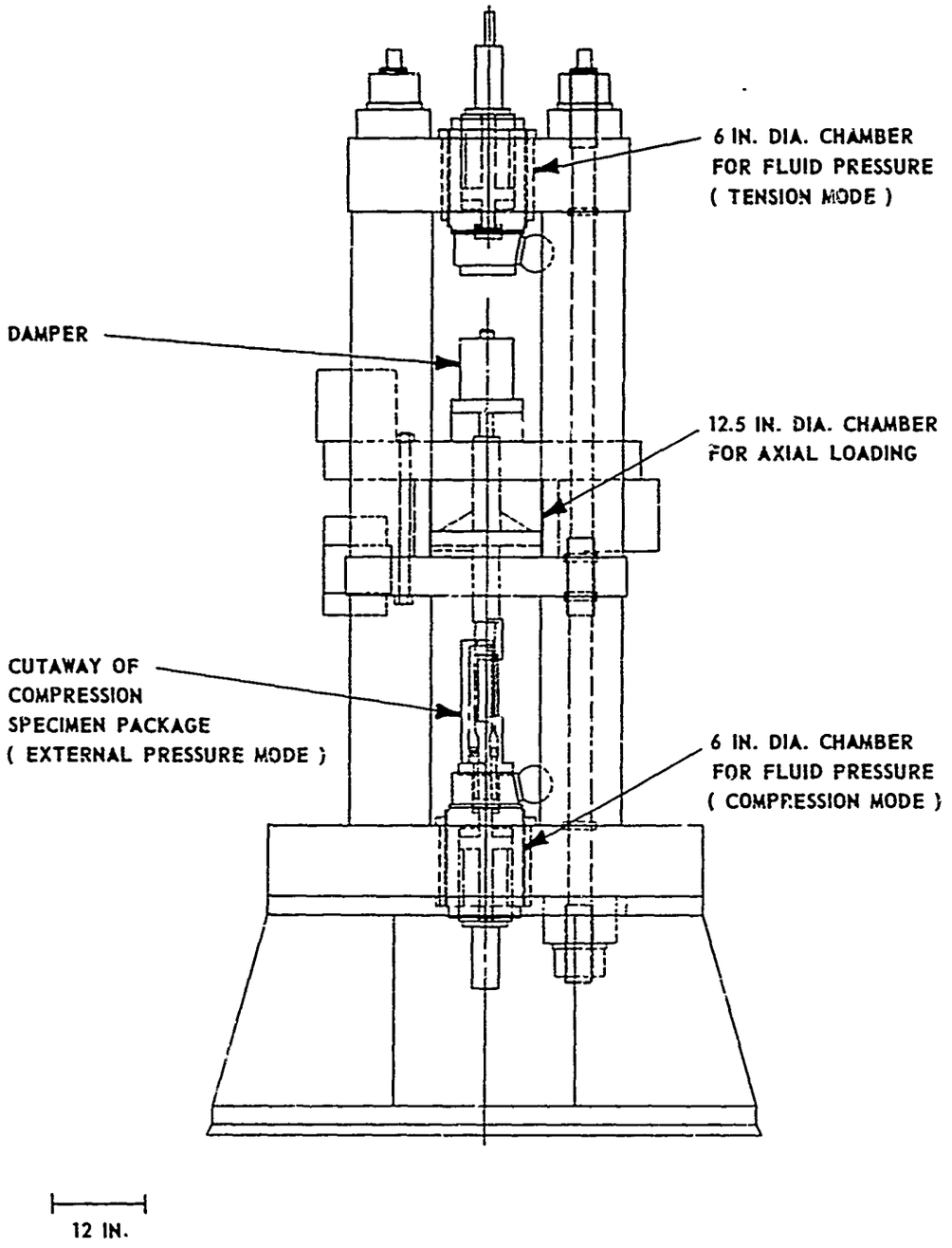

Figure 2 Schematic Diagram of Biaxial Medium Strain-Rate Machine

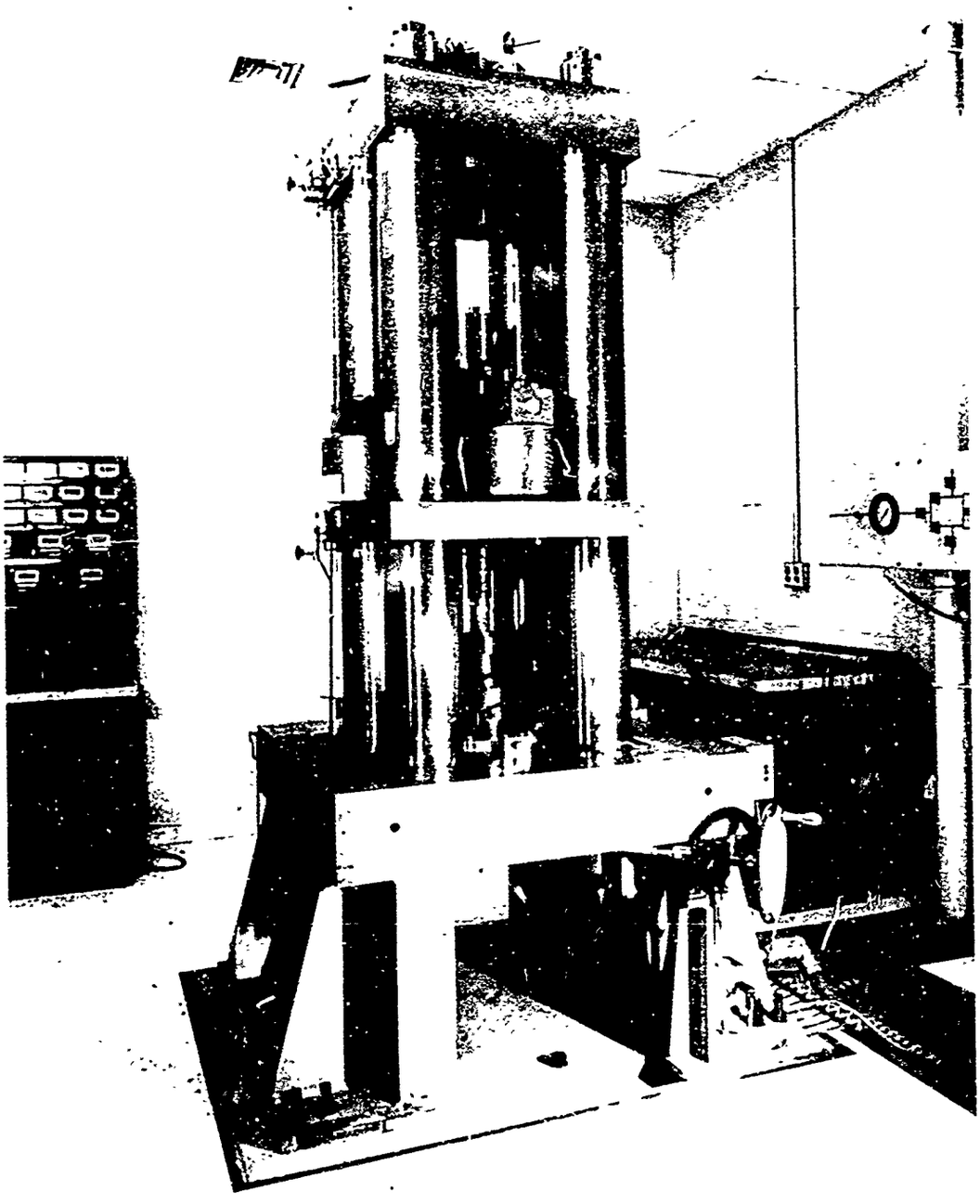

Figure 3 Photograph of Biaxial Medium Strain-Rate Machine

The piston requirements for this machine were based on developing 10% minimum strain on a high strength material with a medium elastic modulus, such as quartz phenolic, at strain rates of 8-10/second. For a 6 inch long specimen tube, the piston must achieve velocities of 50-60 inches/second, and have at least a 0.6 inch stroke to meet these requirements. Additional criteria were low mass, good rigidity, accurate guidance, and high strength.

To predict the proper dimensions based on the above criteria, a mathematical analysis was made of the piston motion as influenced by type and pressure of the gas, piston mass and area, reservoir volumes in front of and behind the piston, and the orifice size. The piston friction, specimen reaction (from uniaxial stress data[46]), and piston damper effect were also included. A schematic of the iteration of the various parameters is shown in Figure 4. The analysis was coded in the Dartmouth Basic language on a General Electric 235 computer. The program computed the velocity and displacement of the piston, and the gas pressure in the small reservoir at incremental times. The complete analysis and typical results are contained in Appendix B. Previous work with the Medium Strain-Rate Machines and comparisons with the preliminary Biaxial Machine Tests have shown good correlation of computed to experimental data.[47]

On the basis of the computer analysis, a 12.5 inch diameter titanium piston was selected for the axial loading source and 6 inch diameter steel pistons were selected to pressurize the fluid. Assuming helium gas at a pressure of 3000 psi, it was determined that velocities of 60 inches/second could be obtained by the 12.5 inch axial loading piston with

quartz-phenolic specimens. Maximum capabilities of the machine are listed in Appendix A.

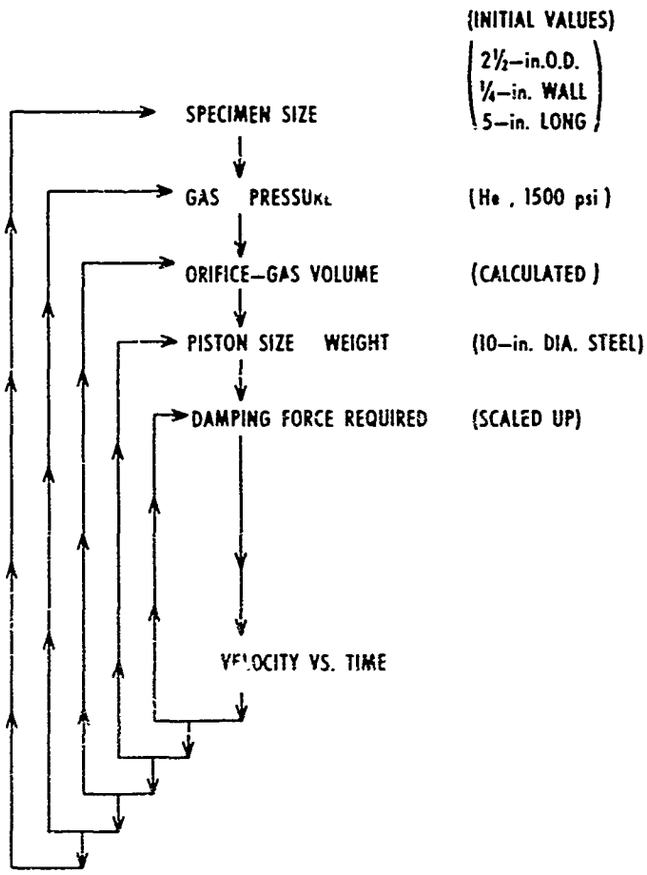

Figure 4 Flow-chart of Parameters Investigated During Piston Motion Study

The 12.5 inch piston was designed to operate in one direction only. Figure 5 shows a cross-section through the cylinder assembly. Note that the piston is braced to increase its stiffness and that the piston stem is hollow to allow a

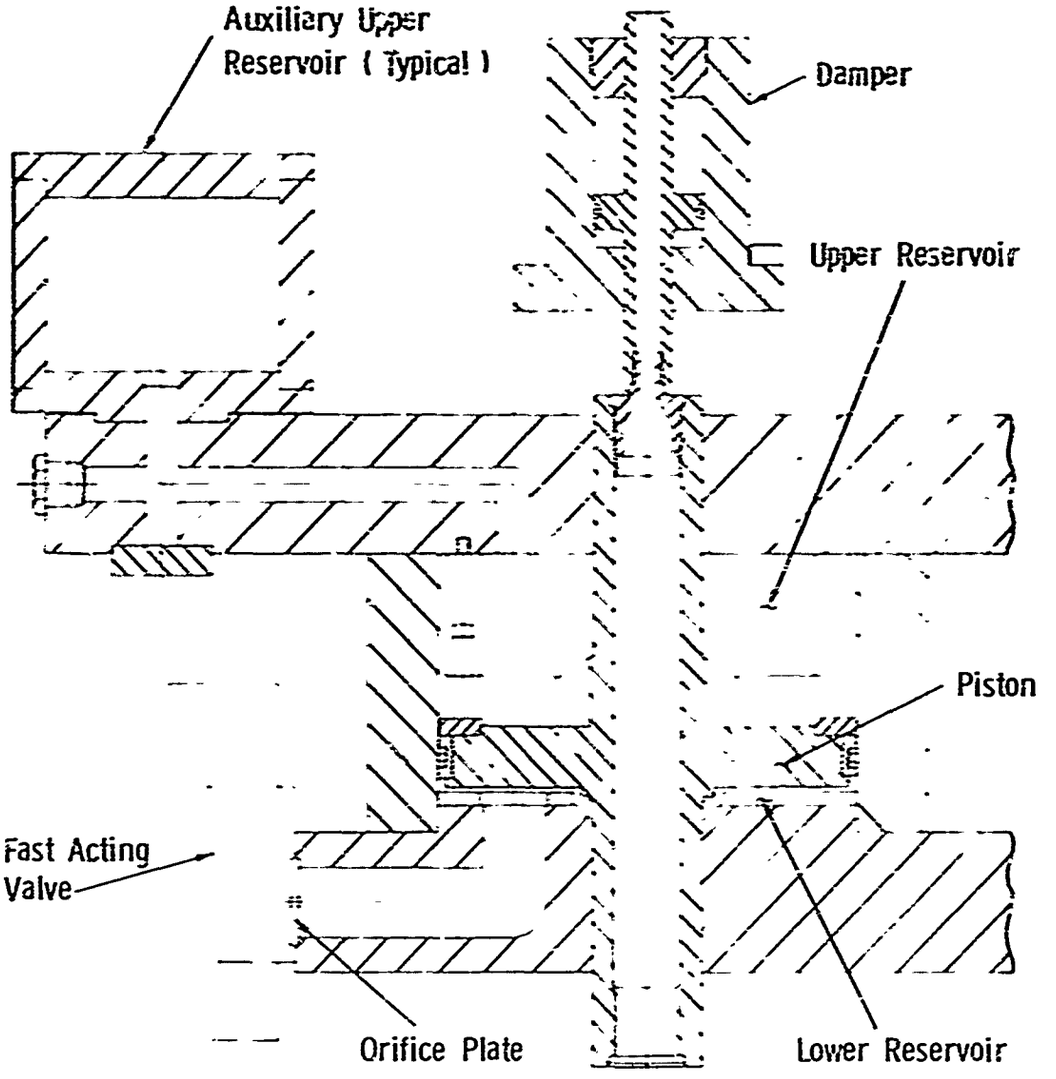

Figure 5 Sectional View of 12.5 inch Diameter, Axial Loading Cylinder

means of egress for instrumentation cables. Because of the unidirectional movement of the piston, the axial compression is obtained on the lower end of the piston and axial tension on the upper end. Because either end of the piston rod may be attached to the specimen for axial loading, the damper assembly also may be connected on either end.

The 6 inch pistons are not braced and may be operated in either direction. (Details of a system similar to that used here may be found in Reference 47). However, because of the unidirectional nature of the axial loading piston, two 6 inch cylinder assemblies were utilized, one for circumferential loading during axial tension and one for circumferential loading during axial compression. Therefore, the 6 inch assemblies effectively operate unidirectionally.

The fast-acting valves connected to the front reservoir of each cylinder provide a means of evacuating the reservoir in minimum time. Between the reservoir and the fast-acting valve is an interchangeable orifice plate which meters the flow of gas from the front reservoir, and thus controls the velocity of the piston.

Figure 6 shows a cross-section through a fast-acting valve. The valve body consists of two chambers. The lower chamber has an entrance port from the main cylinder and an exit port to the exhaust line. The orifice plate is located in the entrance port and a valve plate seals the exit port. The valve plate is connected to the piston in the upper chamber by a piston rod which passes through the chamber wall. Low pressure gas drives the piston and valve plate forward, sealing the exit port. The front reservoir of the main

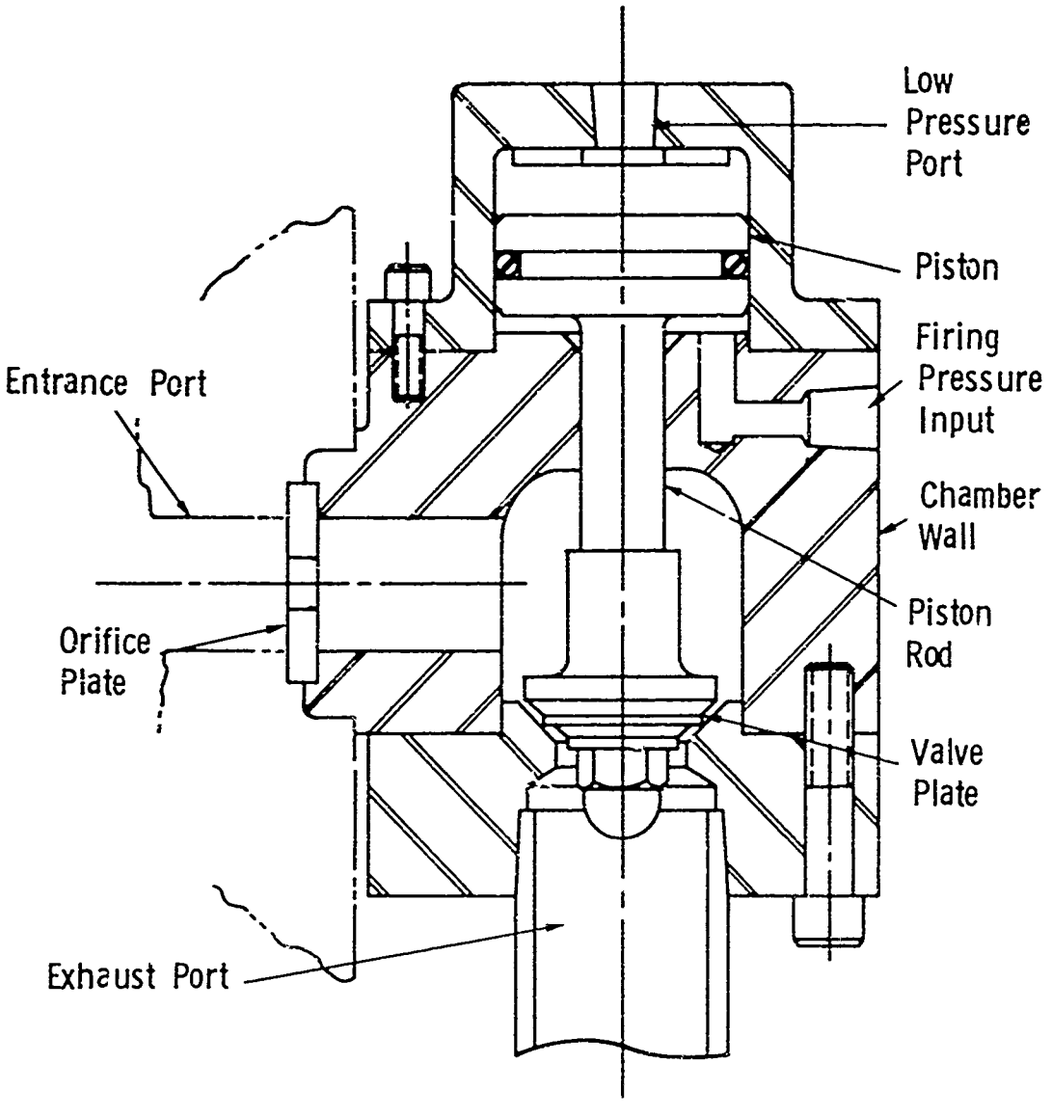

Figure 6 Sectional View of Fast Acting Exhaust Valve

cylinder is now filled with high pressure gas. The high pressure gas acting on the back of the valve plate reinforces the seal. To actuate the valve, high pressure gas is introduced to the front of the piston. Due to the large area of the piston compared to the area of the valve plate, the piston is driven backwards, breaking the exit port seal. The high pressure in the lower chamber then acts on the bottom of the valve plate as well as the top. Because the area under the plate is increased by the area of the rod, the valve plate is accelerated backwards as the high pressure gas flows from the front reservoir of the main cylinder through the orifice plate and out the exit port. The piping diagram for the piston cylinders and the fast-acting valve is shown in Figure 7.

The control panel for the machine is shown in Figure 8. The upper panel controls the 12.5 inch cylinder for all conditions. The lower panel controls either of the two 6 inch cylinders. In addition there is a small panel next to the machine which may operate any of the cylinders (with low pressure air). This panel is used only for setup.

The machine frame was designed to resist separating forces of 400×10^3 lbs. by using prestressed column-and-tie rod construction (shown in Figure 1). The construction is essentially that of two frames with a common middle plate. As only one end of the machine is used at a time, threading the tie rods through the middle plate allows each end of the tie rods to be stressed separately. Calculations (outlined in Appendix C) show deflections of the order of 0.002 inch under maximum rated axial load (340×10^3 lbs.).

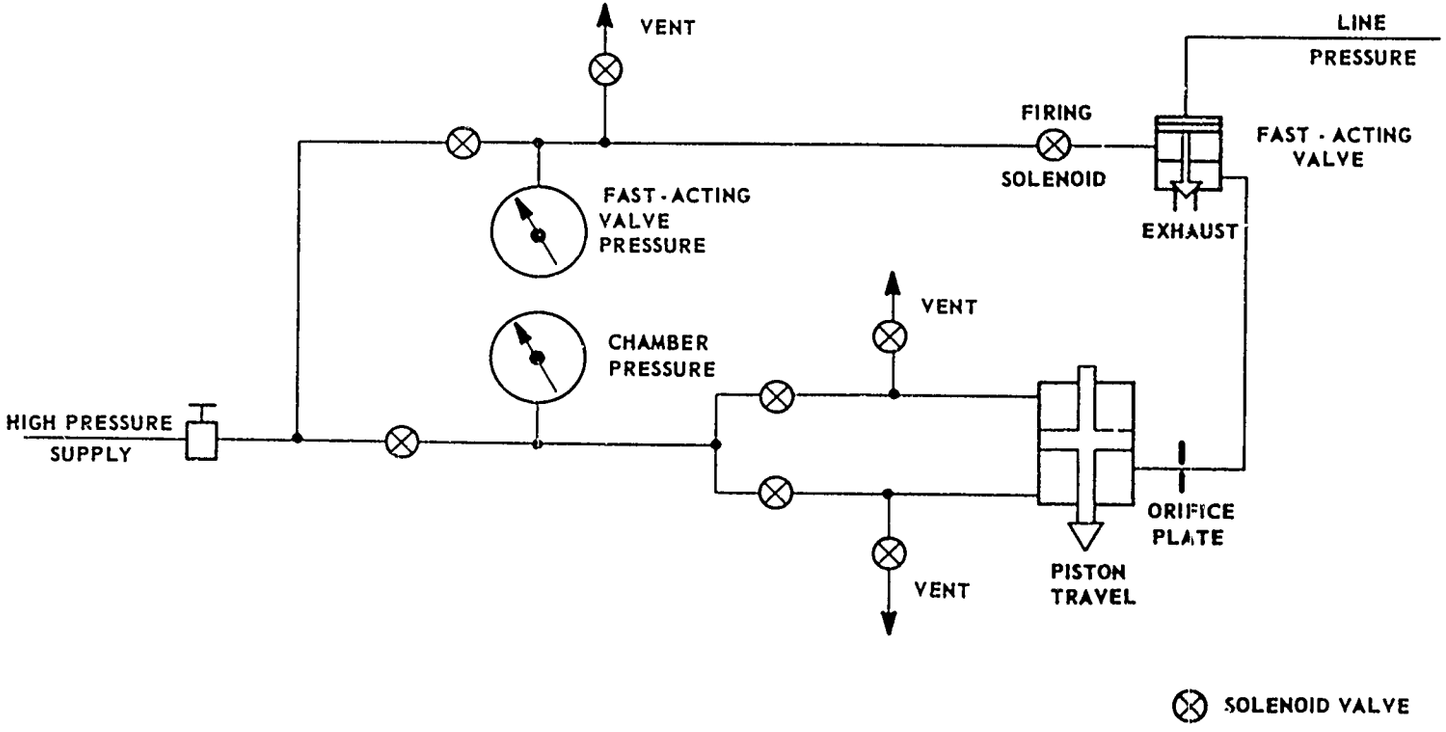

Figure 7 Hydraulic Diagram for Biaxial Machine Loading Cylinder

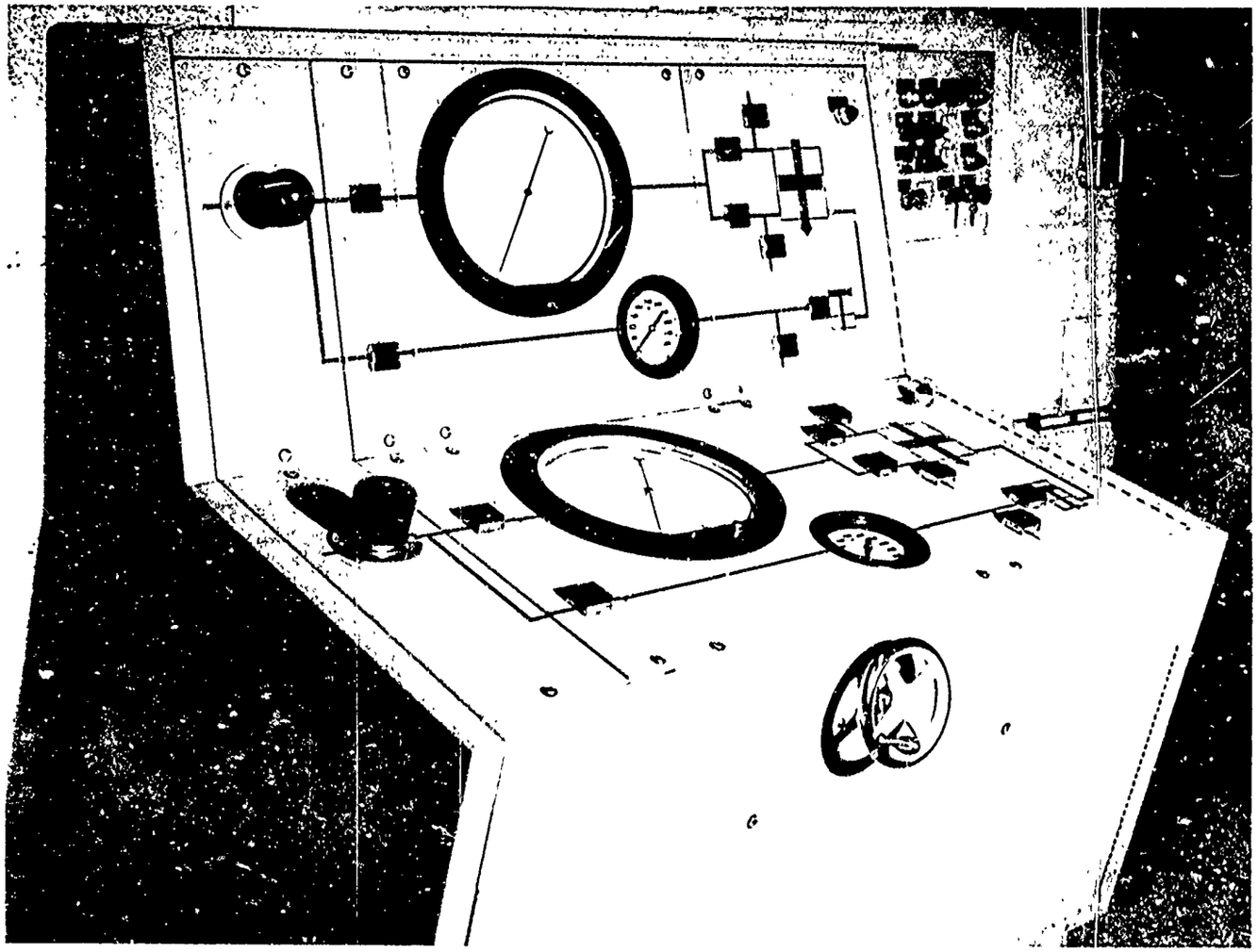

Figure 8 Control Panel for Biaxial Machine

The alignment of the machine, which is necessary to eliminate bending stresses, is very good. The main cylinder and the 6 inch cylinders are on a common axis within 0.002 inch. The frame plates are parallel to within 0.0005 inch (measured between two diagonal columns). Tests on a simulated specimen of steel, instrumented with independently measuring, diagonally opposed, strain gages, showed uniform deformation across the section.

Adjustment for specimen length and preload are made through a positioning mechanism for the 6 inch cylinders (Figure 9). Each cylinder is mounted in a tubular screw threaded into a hollow flanged nut. The nut and screw have buttress threads for maximum load-carrying ability. Axial displacement is effected by rotating the nut by a worm and worm gear while preventing rotation of the cylinder and screw.

The specimen is mounted in a package which serves to support and seal the tubular specimen, to provide a closed pressure chamber, and to provide support for pressure transducers and strain gage seals. Four designs of specimen packages are required to test the four quadrants of the stress plane. Great care is taken in the design of the packages to isolate the axial piston from the action of the pressurized oil in order to insure independent action of the two cylinders.

Figure 10 shows a cross-section through the circumferential tension/axial compression package. A photograph of the assembled package is shown in Figure 11. (All specimen packages are completely assembled outside the machine and installed just prior to a test). The package consists of a

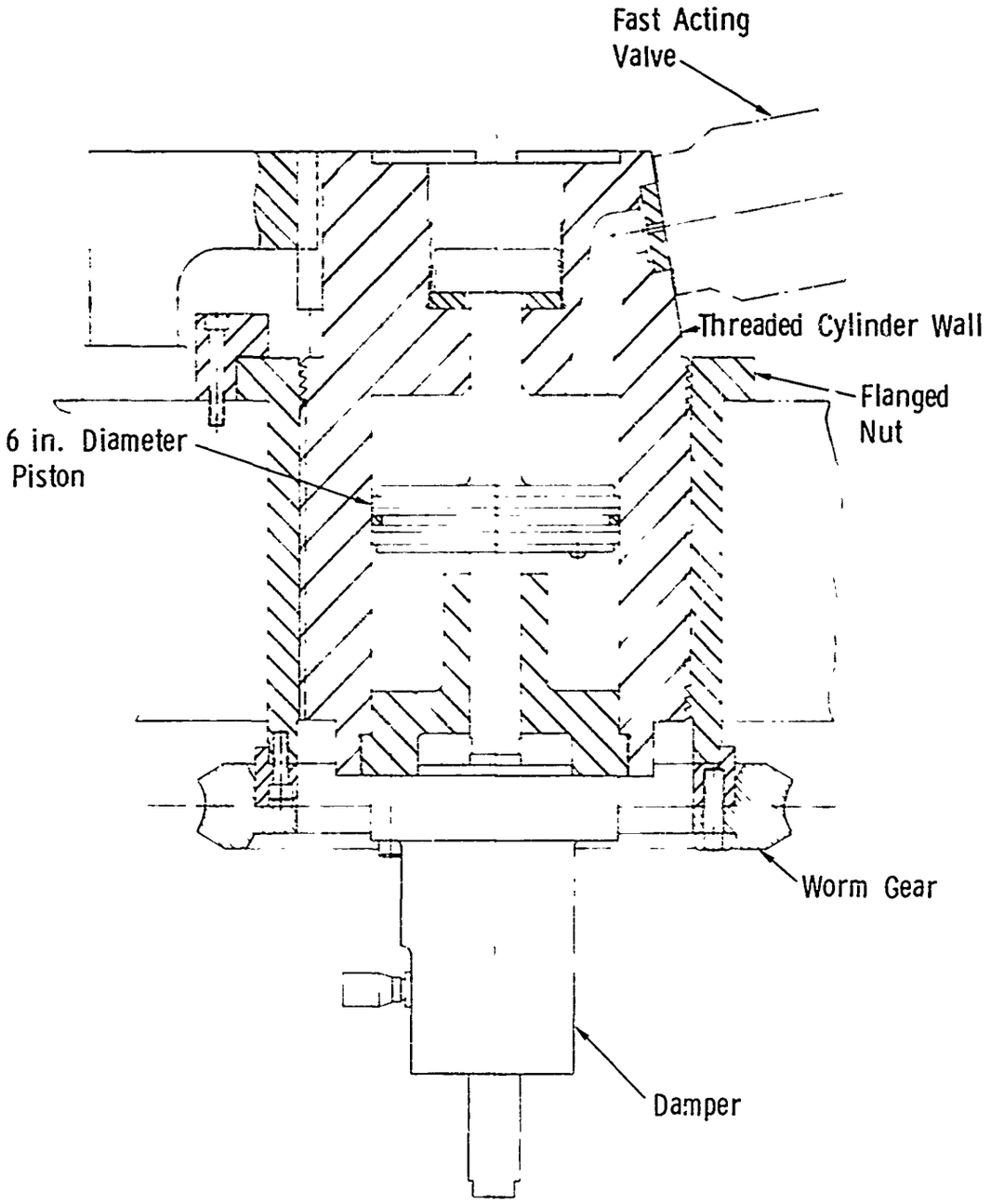

Figure 9 Sectional View of 6 inch Diameter, Circumferential Loading Cylinder

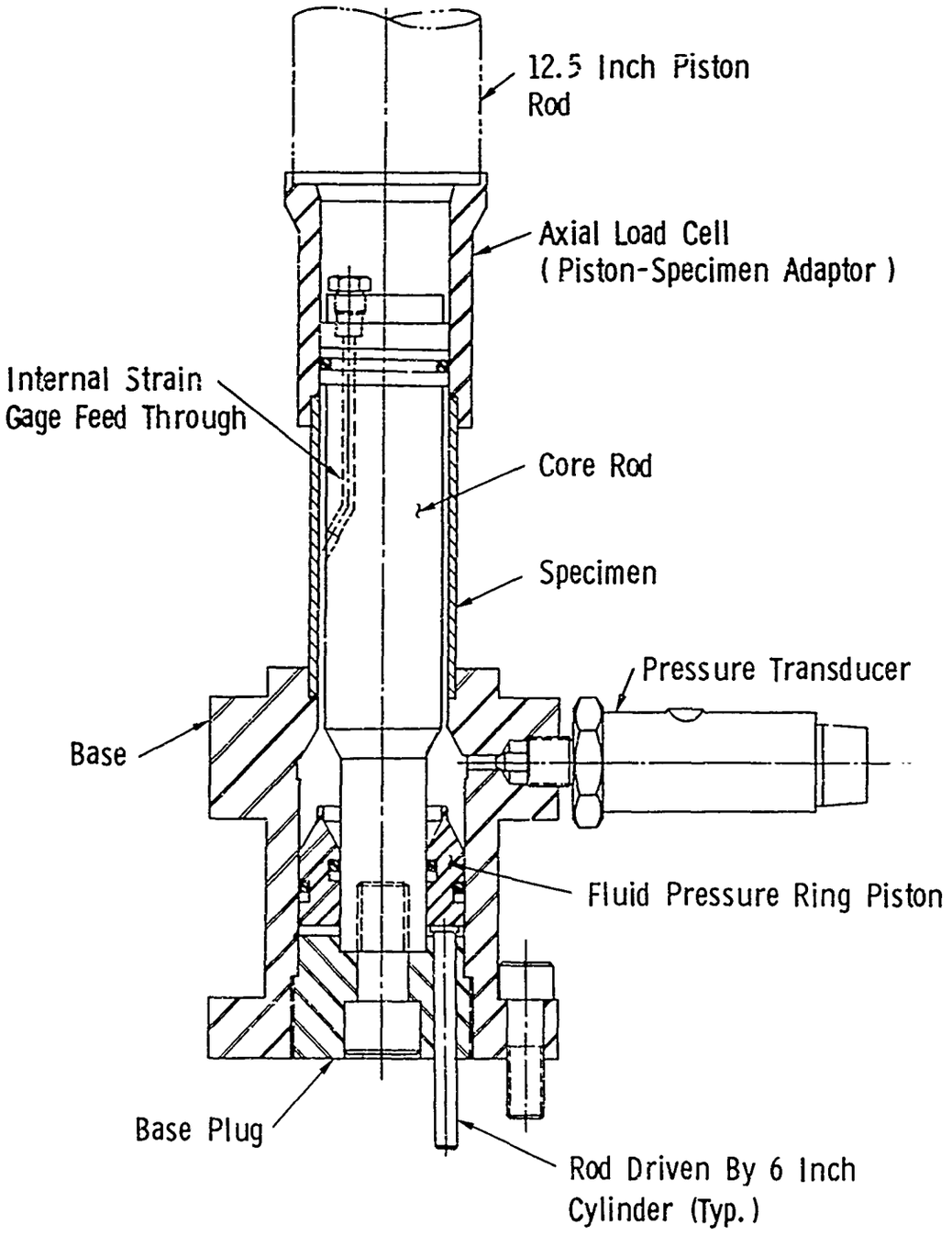

Figure 10 Sectional View of Specimen Package for Axial Compression and Circumferential Tension (Metallic Specimen)

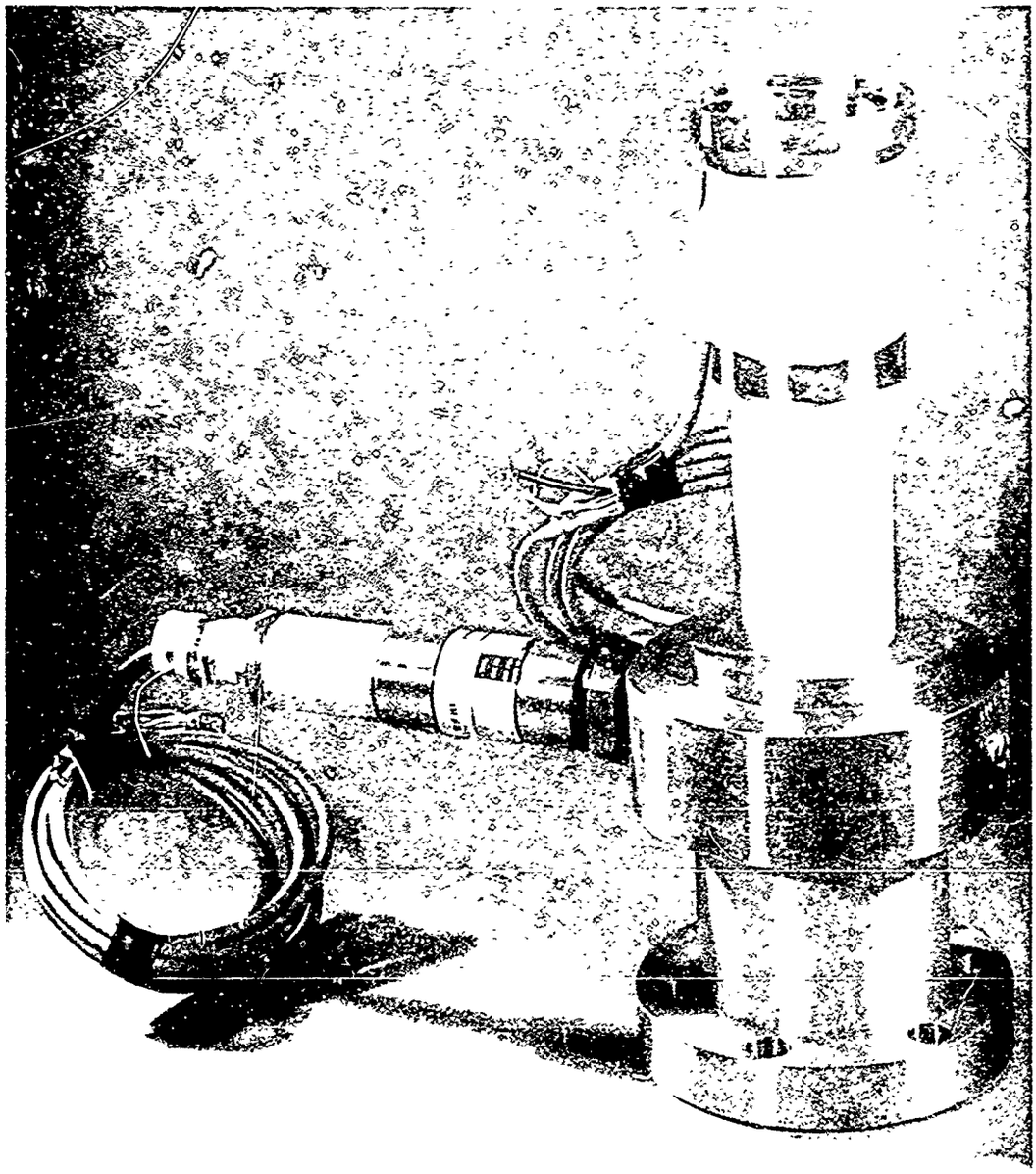

Figure 11 Photograph of a Test Package for Metal Specimens

piston rod adaptor (axial load cell), core rod, tubular specimen, base, ring piston, actuating pins, base plug, and pressure transducer. The specimen is bonded to the piston rod adaptor and the base to seal the internal fluid during assembly and initial portions of a test. The core rod has several functions. It serves to align the assembly, it seals the upper end of the oil chamber, and it reduces the volume of pressurizing fluid required to stress the specimen. Reduction of fluid volume reduces allowable fluid compressibility which, in turn, reduces oil piston stroke requirements.

The nose of the ring piston has a land that cushions the end of its stroke by metering the fluid flow between the base and the core pin. The metering arrangement reduces the possibility of catastrophic piston impact if premature failure of the specimen occurs during a test.

Strain gages may be mounted on both the internal and external surfaces of the specimen. Internal leads for strain gages exit through passages in the core rod. The leads pass through seals at the outer surface, and then through the hollow center of the main piston rod and damper rod.

The external pressure package is identical in operation to the internal package described above. The external load is applied by the fluid contained in an outer steel jacket sealed at both ends. Provisions for stress and strain measurements are similar to those for internal pressure.

SECTION IV

INSTRUMENTATION

Instrumentation for the Biaxial Machine consists of various combinations of load cells, pressure transducers, strain gages, optical extensometers and other transducers. In order to record the many data channels with minimum time skew between channels, a system using a fourteen channel wide band FM tape recorder was assembled.

Figure 12 is a schematic diagram, for a single transducer, of the components involved in the signal conditioning and data recording. The transducer bridge network provides the capability for insertion of a series of parallel calibration resistors (maximum of four), across one active arm in order to electrically simulate test conditions. The bridge network is a Honeywell Accudata 102 which is coupled to a Honeywell Accudata 120 DC amplifier. A null indicator circuit may be connected across any of the fourteen channels to balance the bridge system. From the amplifier, the data are recorded by a fourteen channel, 400 KHz passband, FM tape recorder (Consolidated Electrodynamics Corporation).

This tape system has several advantages over alternate recording systems. One is the very low time skew between any two data channels, one μsecond for this system. Other advantages include continuous recording regardless of the time-of-test, no triggering requirements, high signal to noise ratio, availability of time base expansion and permanent records.

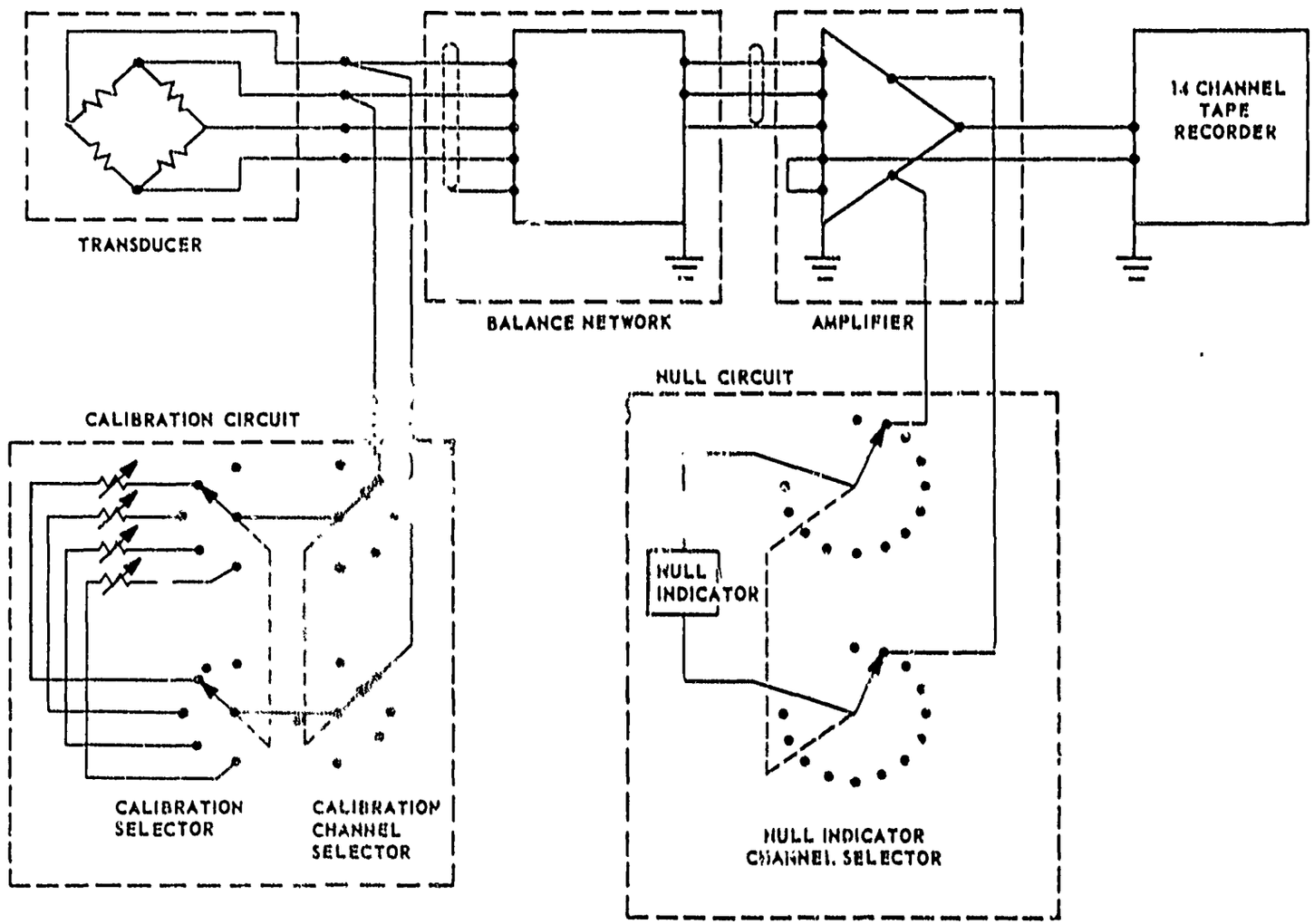

Figure 12 Schematic Diagram of Instrumentation for One Transducer on the Biaxial Machine

Load cells and pressure transducers are calibrated through the system by static loads. Load cells are calibrated against a Morehouse (0.02% accuracy) proving ring while pressure transducers are calibrated against accurate (0.1%) bourdon tube pressure gages. Strain gages are calibrated through the system by electrical simulation only; however, the resistance of each gage is measured just prior to testing to five significant figures in order to achieve maximum accuracy in strain simulation calculations.

The reduction of fourteen channels of data to a computer-compatible form is achieved by direct analog to digital conversion of the data from the analog tape system. The block diagram of the entire system from data sensor to data output is shown in Figure 13. This conversion technique omits all intermediate steps (recording data on film from oscilloscopes, manual digitizing of data, etc.) thereby reducing the cumulative system error as well as retaining the analog data for future reference. The error through this system is approximately ±0.5% of full scale.

The analog to digital (A/D) converter (14 Bit plus sign) used in this system is interfaced to an IBM 1800 central processor. The particular processor used has 16×10^3, 16 bit word storage as well as an associated 5×10^5 word disk storage unit. This flexible system has the capability to digitize, store the data in digital form, input the proper scale factors and print and plot the various reduced data in a usable and convenient form.

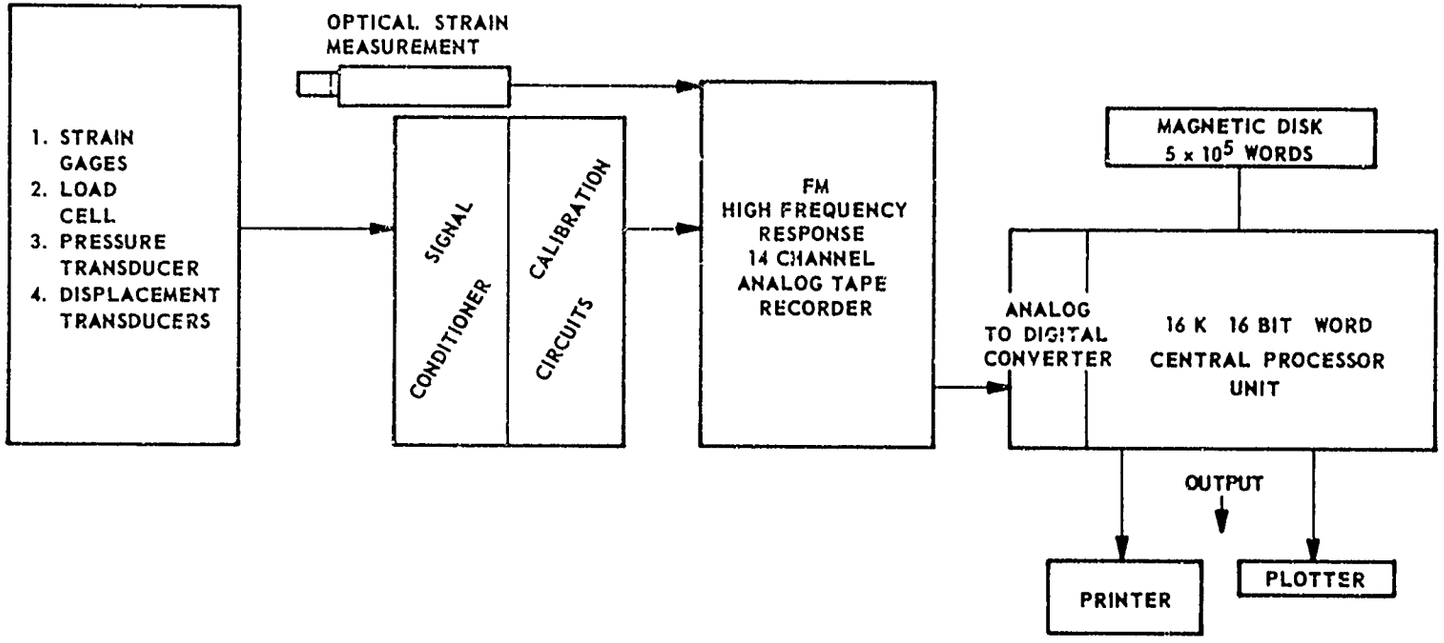

Figure 13 Block Diagram of Data Measurement and Reduction for Biaxial Machine

SECTION V

PRELIMINARY DATA

Initial tests of the Biaxial machine were conducted on 6061-T651 aluminum alloy. This material was purchased in 3 inch diameter rolled rod stock from which test specimens of 2.5 inch O.D. by 2.25 inch I.D. by 5 inch long right circular cylinders were machined. Some additional specimens, 0.375 inch O.D. by 0.500 inch long cylinders, were also fabricated for evaluation by other techniques.

Figure 14 contains data from several tests on the Biaxial machine. Two of the tests are with compressive axial load only and one test is with tensile circumferential load with an axial compressive preload. The behavior of the circumferentially loaded specimen was obtained by using elasticity equations for thick walled tubes and converting internally measured pressure to stress on the outside diameter of the tube, where the strains were measured. Strains greater than 0.75% were not obtained because of loss of gage continuity as the tube expanded. This condition will be remedied in future tests by more flexible lead wire arrangements. As shown, good correlation between the various data was obtained including comparison tests with 0.375 inch diameter by 0.500 inch long samples tested on the Medium Strain-Rate machine. Figure 15 shows a specimen tested in compression only while Figure 16 shows a specimen tested in circumferential tension only.

As shown in Figure 15, these aluminum tubes buckled after about 3% deformation. Although all samples tested in com-

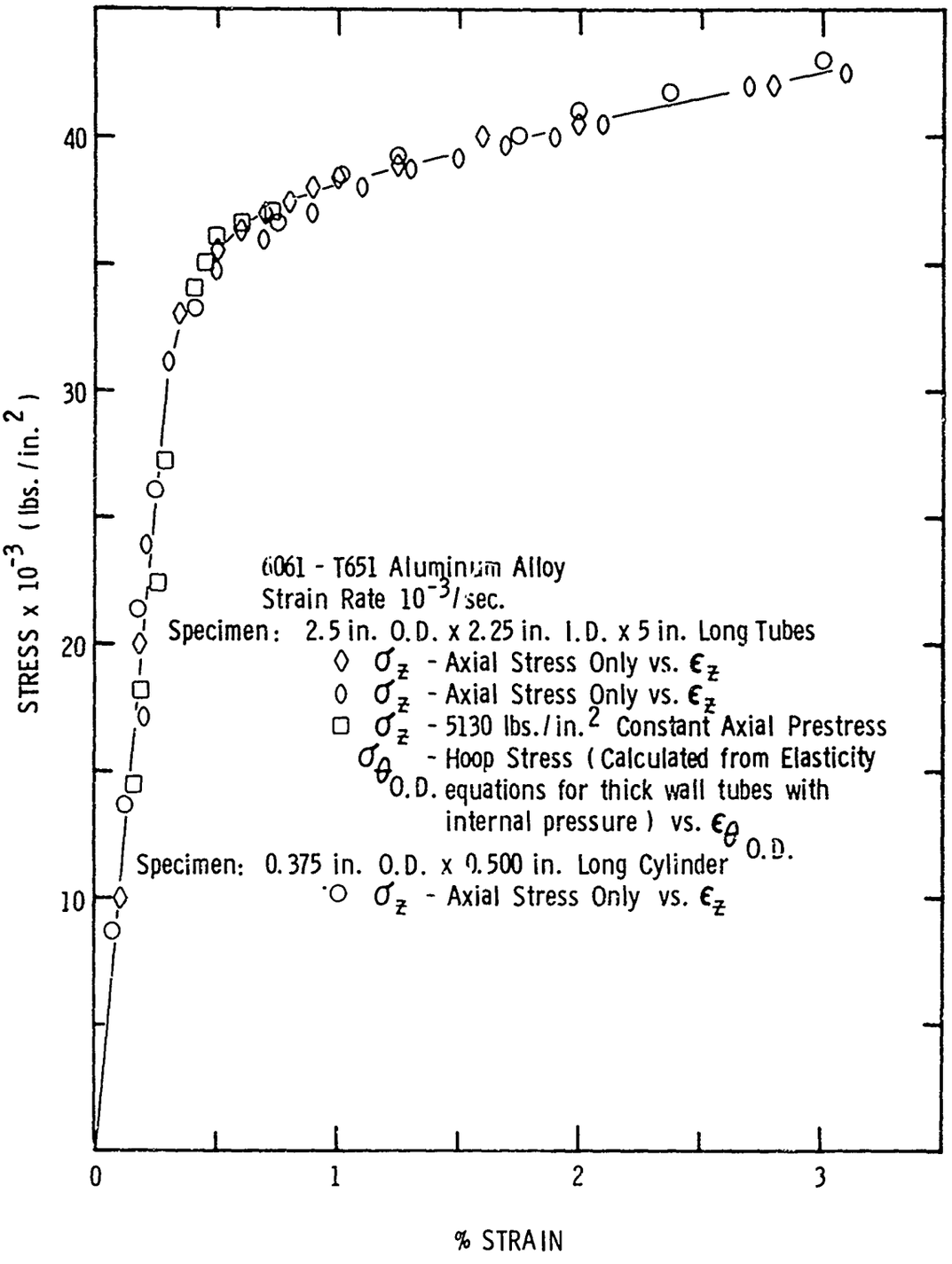

Figure 14 Stress Versus Strain for 6061-T651 Aluminum

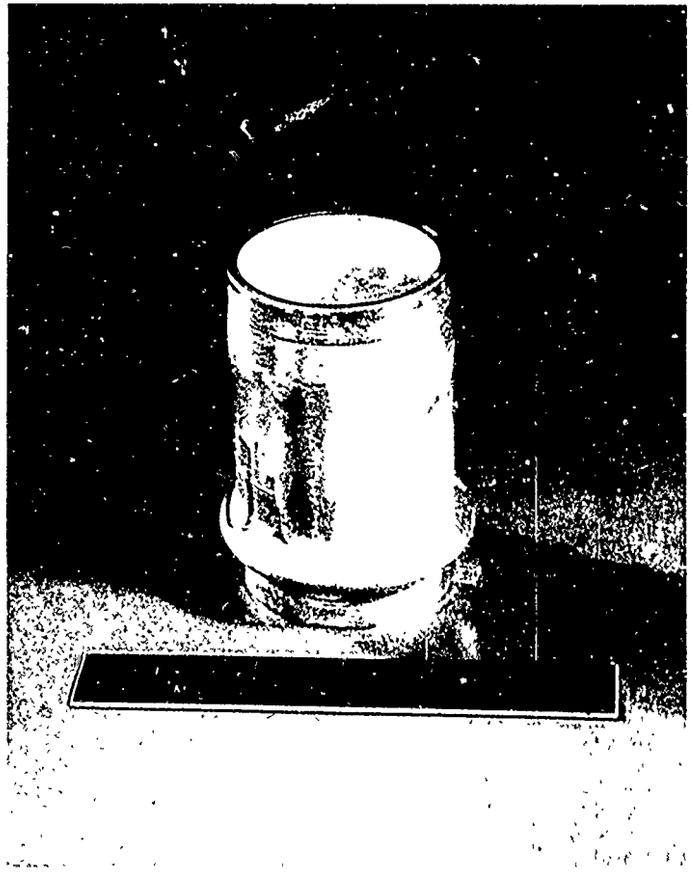

Figure 15 Photograph of Aluminum Tube Tested under Axial Load Only

Figure 16 Photograph of Aluminum Tube Tested under Circumferential Load (With Constant Axial Load)

pression buckled on the lower end of the specimens, incipient buckling (i.e. shown by bulging) occurred on the upper end of the specimens. Figure 17 shows the stress, strain, time data for a specimen instrumented with strain gages at three positions along the outside wall axis and one gage on the inside wall. During the elastic portion, excellent agreement was obtained between all gages. After yield, however, only the center two gages agreed closely. The gages on the extremes departed from the center gages, especially towards the end of the test when the specimen buckled. The specimen load drops at buckling and then remains constant until the end of the test (not shown in the figure). The erratic behavior of the inside center strain gage after 6 seconds into the test is probably the result of the strain gage de-bonding from the specimen.

Figure 18 shows the strain-time behavior for a specimen instrumented as above but loaded with internal pressure only. The data are from the three strain gages on the external surface. Note that only small deviations between gages were recorded. From these data it has been shown that the material behavior in the center of the specimen is not influenced by the end constraints for small deformations.

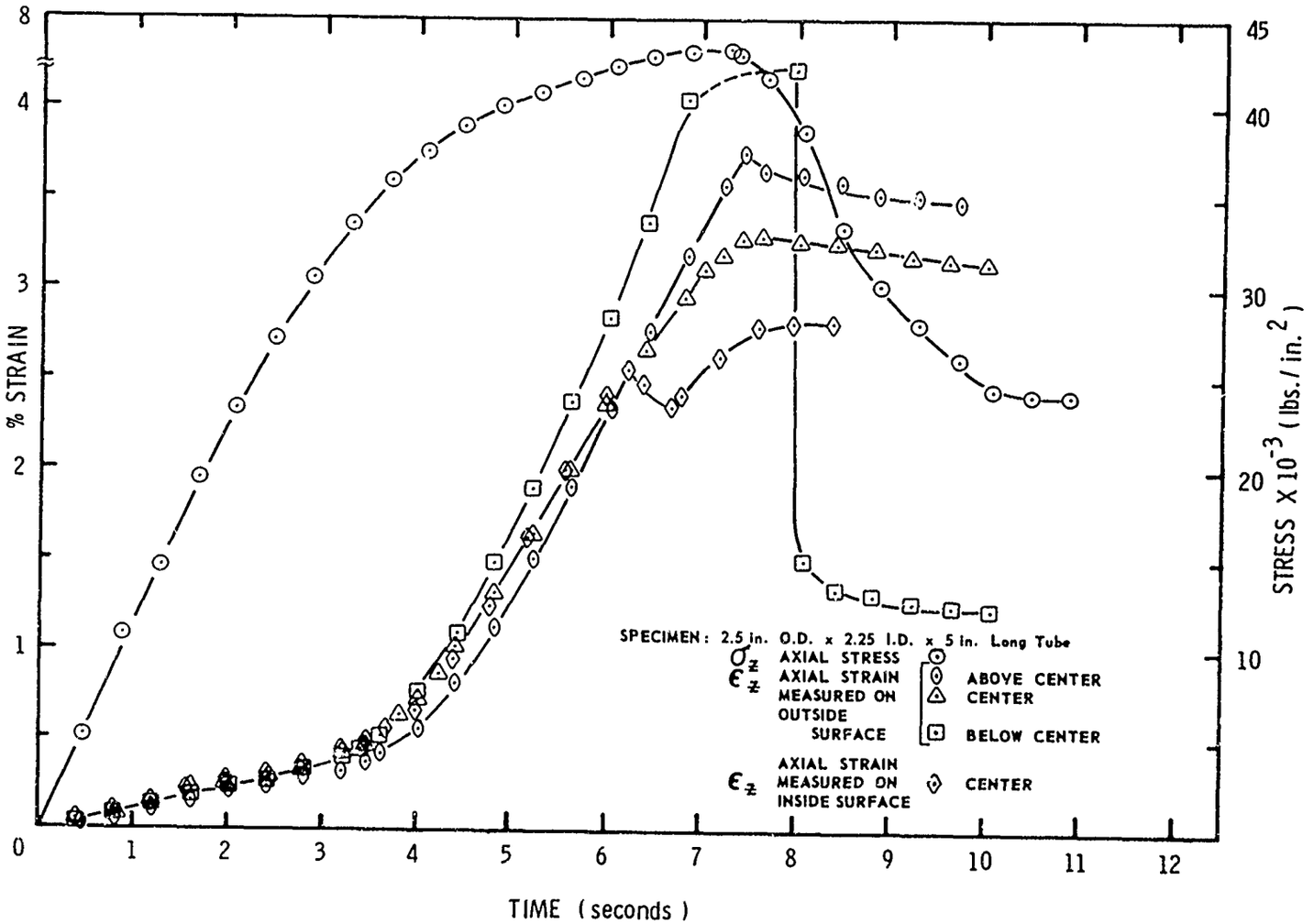

Figure 17 Stress and Strain Versus Time for an Extensively Instrumented Aluminum Tube Under Axial Load Only

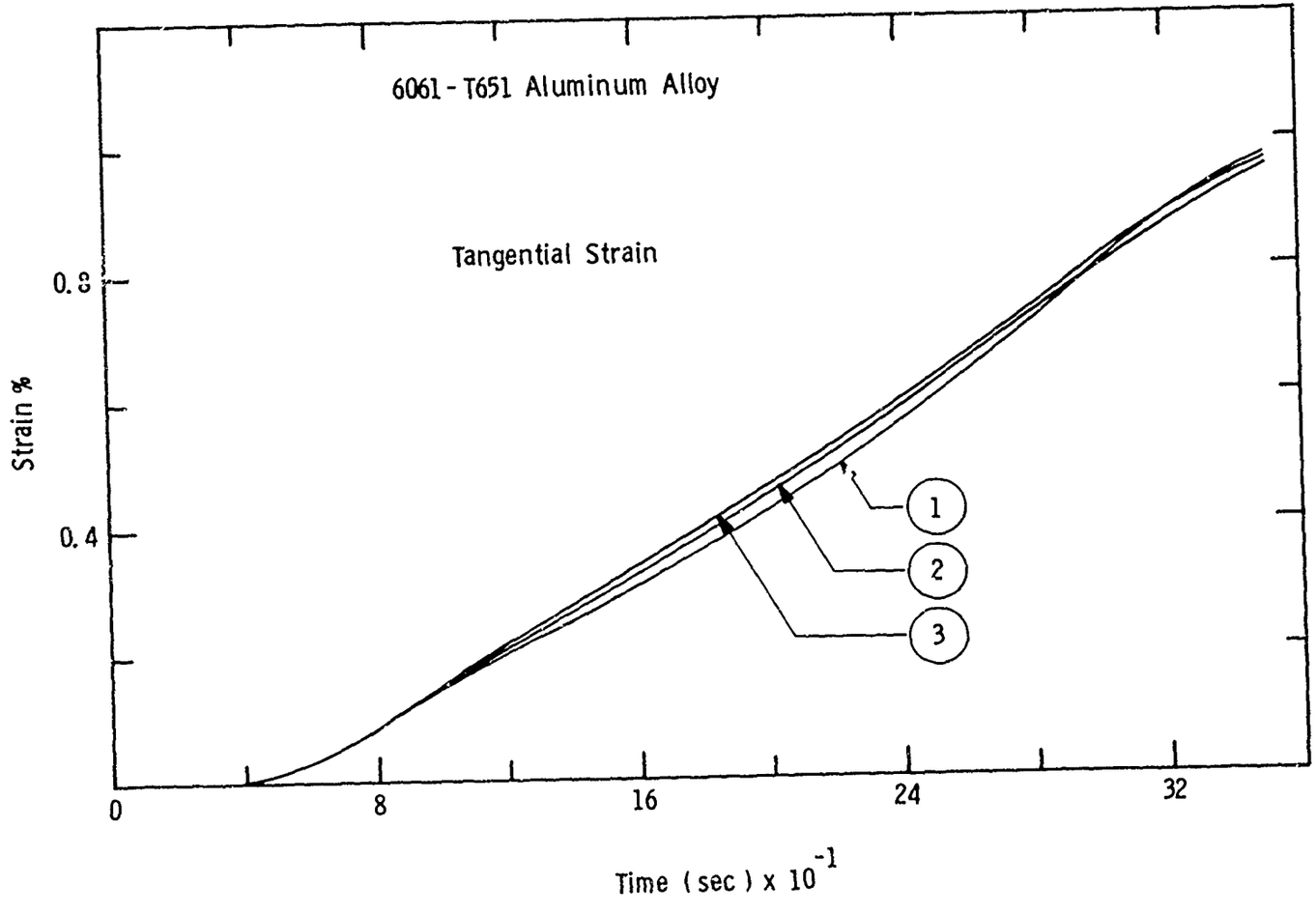

Figure 18 Strain Versus Time at Three Positions Along the Axis of an Aluminum Tube Loaded with Internal Pressure (With Constant Axial Load)

ACKNOWLEDGMENTS

The authors would like to acknowledge the efforts of Mr. T. Lee during the design of the Biaxial Machine, Mr. L. King and Mr. J. Bergamo during its construction and the excellent work of the hydraulic and electrical technicians of Mr. P. Burton during assembly of the machine.

The authors also would like to thank Mr. G. Hopewell and Mr. M. Klewicki for their efforts in collecting data from the machine. Special acknowledgment is accorded Mr. F. Schierloh and Mr. R. Chaney for selecting the hardware and developing the computer routines necessary for reduction of Biaxial Machine data.

REFERENCES

1. A. Nadai and M. Manjoine, "High Speed Tension Tests at Elevated Temperature-Parts I and II", J. App. Mech., Vol. 8, June, 1941.

2. H. Kolsky, "An Investigation of the Mechanical Properties of Materials at Very High Rates of Loading", Proc. of the Physical Society, Section B, Vol. 62, 1949.

3. D. S. Clark and D. S. Wood, "The Time Delay for the Initiation of Plastic Deformation at Rapidly Applied Constant Stress", Proc. ASTM, Vol. 49, 1949.

4. J. D. Campbell, "An Investigation of the Plastic Behavior of Metal Rods Subjected to Longitudinal Impact", J. Mech. Physics of Solid, Vol. I, 1953.

5. J. M. Krafft, A. M. Sullivan, and C. F. Tipper, "The Effect of Static and Dynamic Loading and Temperature on the Yield Stress of Iron and Mild Steel in Compression", Proc. of the Royal Society, Series A, Vol. 221, 1954.

6. E. D. H. Davies and S. C. Hunter, "The Dynamic Compression Testing of Solids by the Method of the Split Hopkinson Pressure Bar", J. Mech. Physics of Solids, Vol. II, 1963.

7. J. E. Johnson, D. S. Wood, and D. S. Clark, "Dynamic Stress-Strain Relations for Annealed 2S Aluminum Under Compression Impact", J. App. Mech., Vol. 20, 1953.

8. J. D. Campbell and C. J. Maiden, "The Effect of Impact Loading on the Static Yield Strength of a Medium-Carbon Steel", J. Mech. Physics of Solids, Vol. 6, 1957.

9. J. L. Chiddister and L. E. Malvern, "Compression-Impact Testing of Aluminum at Elevated Temperatures", Exp. Mech. Vol. 3, April, 1963.

10. C. J. Maiden and S. J. Green, "Compressive Strain-Rate Tests on Six Selected Materials at Strain Rates from 10^{-3} to 10^{4} in/in/sec.", J. App. Mech., Vol. 33, Sept., 1966.

11. C. H. Karnes and E. A. Ripperger, "Strain Rate Effects in Cold Worked High Purity Aluminum", J. Mech. Physics of Solids, Vol. 14, 1966.

12. F. E. Hauser, J. A. Simmons, and J. E. Dorn, Response of Metals to High Velocity Deformation, Ed. by V. F. Zackay, Interscience, N.Y., 1961.

13. U. S. Lindholm, "Some Experiments with the Split Hopkinson Pressure Bar", J. Mech. Physics of Solids, Vol. 12, 1964.

14. S. J. Green and R. D. Perkins, "Uniaxial Compression Tests at Strain Rates from 10^{-4}/second to 10^{4}/second on Three Geologic Materials", Presented at 10th Symposium on Rock Mechanics, Austin, Texas, May 1968.

15. U. S. Lindholm and L. M. Yeakley, "A Dynamic Biaxial Testing Machine", Exp. Mech., Vol. 7, Jan., 1967.

16. G. Gerard and R. Papirno, "Dynamic Biaxial Stress-Strain Characteristics of Aluminum and Mild Steel", Trans. of ASM, Vol. 49, 1967.

17. K. G. Hoge, "The Influence of Strain Rate on Mechanical Properties of 6061-T6 Aluminum Under Uniaxial and Biaxial States of Stress", Exp. Mech., Vol. 6, April, 1966.

18. J. D. Chalupnik and E. A. Ripperger, "Dynamic Deformation of Metals Under High Hydrostatic Pressure", Experimental Mechanics, Vol. 6, November, 1966.

19. G. R. Fowles, "Shock Wave Compression of Hardened and Annealed 2024 Aluminum", J. of Applied Physics, Vol. 32, p. 1475-1487, 1961.

20. C. D. Lundergan and W. Herrmann, "Equation of State of 6061-T6 Aluminum at Low pressures", J. of Applied Physics, Vol. 34, No. 7, p. 2046-2052, 1963.

21. L. M. Barker, C. D. Lundergan and W. Hermann, "Dynamic Response of Aluminum", J. of Applied Physics, Vol. 35, No. 4, p. 1203-1212, 1964.

22. W. Herrmann, E. A. Witmer, J. H. Percy and A. H. Jones, "Stress Wave Propagation and Spallation in Uniaxial Strain", Air Force Systems Command, Tech. Doc. Report No. ADS-TDR-62-399, 1962.

23. C. H. Karnes, "The Plate Impact Configuration for Determining Mechanical Properties of Materials at High Strain Rates", Symposium on the Mechanical Behavior of Material Under Dynamic Loads, San Antonio, Texas, Sept., 1967.

24. A. H. Jones, C. J. Maiden, S. J. Green, and H. Chin, "Prediction of Elastic-Plastic Wave Profiles in Aluminum 1060-0 [illegible]er Uniaxial Strain Loading", Symposium on the Mechani[illegible] Behavior of Material Under Dynamic Loads, San Antonio, Texas. Sept., 1967.

25. E. A. Davis, "Increase of Stress with Permanent Strain and Stress-Strain Relations in the Plastic State for Copper Under Combined Stresses", Trans. ASME, Vol. 65, Dec., 1943, "Yielding and Fracture of Medium-Carbon Steel Under Combined Stress", J. App. Mech., Vol. 12, March, 1945.

26. W. R. Osgood, "Combined-Stress Tests on 24S-T Aluminum-Alloy Tubes", Trans. ASME, Vol. 69, June, 1947.

27. E. G. Thomsen, D. M. Cunningham and J. E. Dorn, "Fracture of Some Aluminum Alloys Under Combined Stress", Trans. ASME, Vol. 69, February, 1947.

28. S. J. Praenkel, "Experimental Studies of Biaxially Stressed Mild Sceel in the Plastic Range", J. App. Mech., Vol. 15, Sept., 1948.

29. J. Marin, L. W. Hu, and J. P. Hamburg, "Plastic Stress-Strain Relations of Alcoa 14S-T6 for Variable Biaxial Stress Rations", Trans ASM, Vol. 45, 1952, also J. Marin and L. W. Hu, "Biaxial Plastic Stress-Strain Relations of Mild Steel for Variable Stress Ratios", Trans ASME, Vol. 78, April, 1956.

30. W. N. Findley and A. Gjelsvik, "A Biaxial Testing Machine for Plasticity, Creep, or Relaxation Under Variable Principle-Stress Ratios", Proc. Am. Soc. for Testing and Materials, 1962, also P. K. Bertsch and W. H. Findley, "An Experimental Study of Subsequent Yield Surfaces-Corners, Normality, Bauschinger, and Allied Effects", Proceedings of 4th National Congress of Applied Mechanics, 1962.

31 H. Ll. D. Pugh, W. M. Mair, and A. C. Rapier, "An Apparatus for Combined Testing in the Plastic Range", Proc. SESA, Vol. 21, 2, Oct., 1964.

32. B. H. Jones, "Assessing Instability of Thin-Walled Tubes Under Biaxial Stresses in the Plastic Range", Exp. Mech., Vol. 8, Jan., 1968, also B. H. Jones and P. B. Mellor, "Plastic Flow and Instability Behavior of Thin-Walled Cylinders Subjected to Constant-Ratio Tensile Stress", J. of Strain Analysis, Vol. 2, No. 1, 1967.

33. I. Cornet and R. C. Grassi, "A Study of Theories of Fracture Under Combined Stresses", Trans ASME, J. Basic Engr., Vol. 83, March, 1961.

34. R. E. Ely, "Strength of Graphite Tube Specimens Under Combined Stresses", J. of American Ceramic Society, Vol. 48, Oct., 1965.

35. H. M. Babel and G. Sines, "A Biaxial Fracture Criteria for Porous Brittle Materials", Trans-ASME, J. Basic Engr., Vol. 90, June, 1968.

36. A. Nadai and L. H. Donnell, "Stress Distribution in Rotating Discs of Ductile Material After the Yield Point Has Been Reached", Trans ASME, 1916.

37. A. M. Wahl, G. O. Sankey, M. J. Manjoine, and E. Shoemaker, "Creep Tests of Rotating Discs at Elevated Temperature and Comparison with Theory", J. App. Mech., Vol. 21, Sept., 1954.

38. A. E. Johnson, "Creep Under Complex Stress Systems at Elevated Temperatures", Proc. of the Institute of Mech. Engrs., Vol. 164, 1951, p. 432.

39. E. Shiratori and K. Ikegami, "A New Biaxial Tensile Testing Machine with Flat Specimen", Bulletin of the Tokyo Institute of Technology, No. 82, 1967.

40. M. J. Manjoine, "Biaxial Brittle Fracture Tests", Trans of ASME, J. Basic Engr, Vol. 86, 1964.

41. P. W. Bridgman, "Studies in Large Plastic Flow and Fracture", Harvard University Press, 1964.

42. H. Ll. D. Pugh and D. A. Gunn, "An Apparatus for Torsion Tests Under High Hydrostatic Pressure", Proceedings of ASME Symposium on High Pressure Technology, 1964.

43. J. Handin, "An application of high pressure in geophysics: Experimental Rock Deformation", Trans. of ASME, Vol. 75, p. 315-324, 1953.

44. D. T. Griggs, "Deformation of Rocks Under High Confining Pressures", Journal of Geological Research, Vol. 44, p. 541-577, 1936.

45. J. Logan, (Private Communication), Center for Tectonophysics, Texas A & M University, College Station, Texas, May, 1968.

46. S. J. Green, S. G. Babcock, and R. D. Perkins, "Final Report, Fundamental Material Behavior Study, Vol. 1, Responses of Several Reentry Vehicle Materials to Impulsive Loads", BSD-TR-67-23, February, 1967.

47. C. J. Maiden, et. al., "Response of Materials to Suddenly Applied Stress Loads" (Interim Report) DASA-1716, Oct., 1965.

APPENDIX A

SPECIFICATIONS FOR BIAXIAL MACHINE

I. Axial-Load Piston

Diameter = 12.5 in
Effective Area = 114 in^2
Mass = 0.146 lb - sec^2/in
Max. Gas Pressure = 3000 psi
Gas Type = Air, Helium, Nitrogen
Max. Force @ 3000 psi = 342,000 lbs
Max. Travel = 1.76 in
Max. Force @ End of 1.76 in. Travel = 263,000 lbs
Material = Titanium
Gas Volume = 1212 in^3

II. Circumferential-Load Piston

Diameter = 6.0 in
Effective Area = 27 in^2
Mass = 0.046 lb - sec^2/in
Max. Gas Pressure = 3000 psi
Gas Type = Air, Helium, Nitrogen
Max. Force @ 3000 psi = 81,000 lbs
Max. Travel = 2.0 in
Max. Force @ End of 2.0 in. Travel = 37,000 lbs
Material = Steel
Gas Volume = 127 in^3

III. Biaxial Compression Specimen

Max. Length = 10 in
Max. O.D. = 4 in
Max. Working Height = 18 in } Specimen
Max. Working Dia. = 9 in } Package
Max. Access Dia. = 12 in

IV. Biaxial Tension Specimen

Max. Length = 11 in
Max. O.D. = 4 in
Max. Working Height = 21 in } Specimen
Max. Working Dia. = 9 in } Package
Max. Access Dia. = 12 in

V. Machine

O.D. Height = 11 ft
Base Area = 20 sq ft
Weight ≅ 1900 lbs
Column Preload = 400,00 lbs (Total)
Max. Frame Deflection at 340,000 lb
Load = 0.002 in

APPENDIX B

ANALYTICAL STUDY OF PISTON MOTION

The assumptions made in the derivation and solution of the equations of piston motion are as follows:

a. The small and large reservoir pressures and volumes are functions of time.
b. An isentropic expansion occurs in the small reservoir and sonic flow exists in the orifice.
c. Such constants as orifice coefficient and friction forces on the piston can be found by comparing analytical results with the results of actual tests.
d. The specimen force can be approximated by a series of linear load-displacement curves.

Definitions -

V_I = Initial volume of small reservoir (in^3)
V_1 = Volume of small reservoir (in^3)
V_{3I} = Initial Volume of large reservoir (in^3)
V_3 = Volume of large reservoir (in^3)
P_I = Initial gas pressure in reservoirs (psi)
P_1 = Gas pressure in small reservoir (psi)
P_2 = Gas pressure in orifice throat (psi)
P_3 = Gas pressure in large reservoir (psi)
d = Diameter of orifice (in)
A = Effective area of piston (in^2)
A_2 = Area of orifice (in^2)

M = Mass of piston (lb-sec^2/in)

F_1 = Friction force (lb)

F_2 = Specimen force (lb)

F_3 = Damping force (lb)

a = Acceleration of piston (in/sec^2)

S = Displacement of piston (in)

S_I = Initial position of piston (in)

K = Ratio of specific heats

C_p = Specific heat at constant pressure (BTU-lb/°R)

R = Universal Gas Constant (ft-lb/lb-°R)

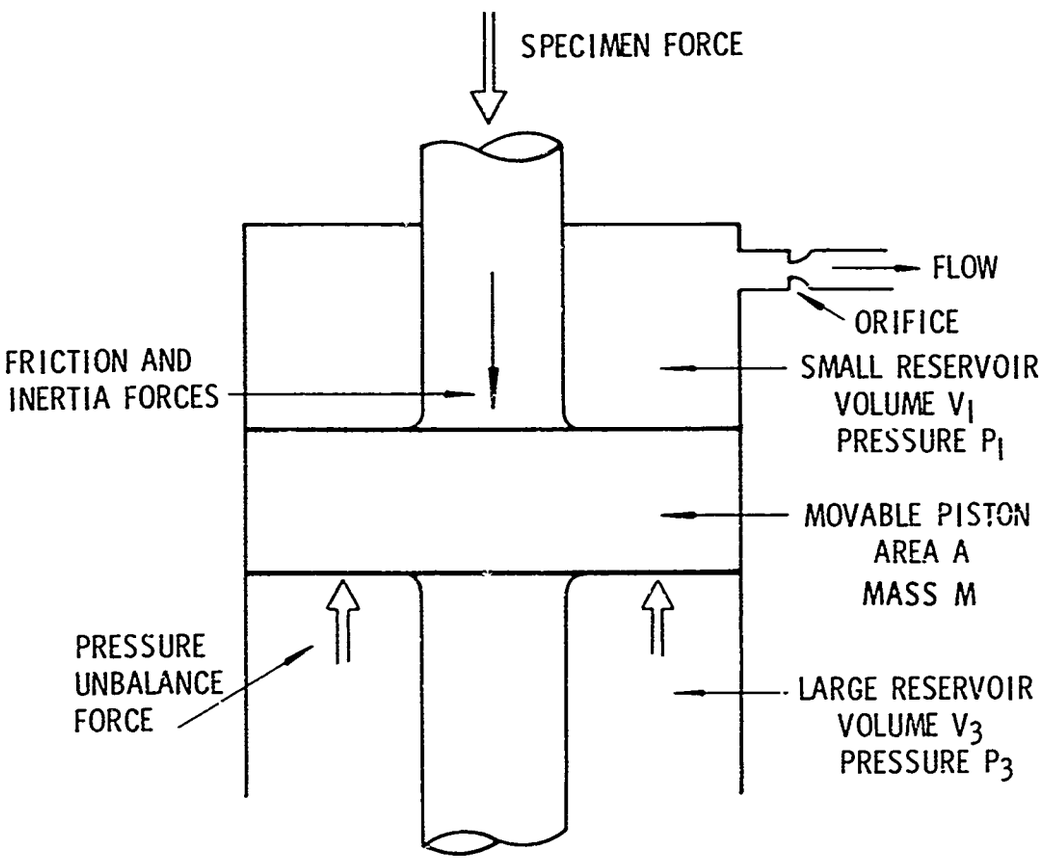

Figure B-1 Force System for Piston Motion Study

1. Balancing forces -

$$Ma = (P_3-P_1)\ A - F_1-F_2-F_3$$

$$a = \frac{1}{M}\left[A(P_3-P_1) - F_1-F_2-F_3\right]$$

Critical pressure in orifice throat -

$$P_2 = P_1\left[\frac{2}{k+1}\right]^{\frac{k}{k-1}} \qquad \text{(Sonic velocity)}$$

$$\frac{P_2}{P_1} = 0.528 \qquad \text{(For air)}$$

2. Initial temperature -

$$T_I = 530°R$$

$$T_1 = T_I\left[\frac{P_1}{P_I}\right]^{\frac{k-1}{k}}$$

Let

$$g = \frac{P_1}{P_I}$$

(ratio of pressure to initial pressure in small reservoir)

Then -

$$T_1 = T_I\, g^{\frac{k-1}{k}}$$

3. Determination of P_1-

The mass flow rate of an ideal fluid through an orifice is:

$$W_f = 223.8 \frac{A_2 P_1}{R} \left\{ \frac{C_p}{T_1} \left[\left(\frac{P_2}{P_1} \right)^{\frac{2}{k}} - \left(\frac{P_2}{P_1} \right)^{\frac{k+1}{k}} \right] \right\}^{\frac{1}{2}} \text{ lb/sec}$$

where -

P_1 = Pressure in small reservoir (lbs/in^2)
T_1 = Temperature of air in orifice (°R)
A_2 = Area of the Orifice (in^2)

and for air -

K = 1.4
C_p = 0.24 BTU-lb/°R
R = 53.3 ft-lb/lb-°R

Substituting and rearranging -

$$W_f = 223.8 \left(\frac{\pi d^2}{4} \right) \left(\frac{P_I}{R} \right) \left(\frac{P_1}{P_I} \right) \left\{ \frac{C_p}{T_I \left(\frac{P_1}{P_I} \right)^{\frac{k-1}{k}}} \left[(0.528)^{\frac{2}{k}} - (0.528)^{\frac{k+1}{k}} \right] \right\}^{\frac{1}{2}} \text{ lb/sec}$$

Let:

$$\alpha_1 = 223.8 \left(\frac{\pi d^2}{4}\right) \frac{P_I}{R} \left\{ \frac{C_p}{T_I} \left[(0.528)^{\frac{2}{k}} - (0.528)^{\frac{k+1}{k}} \right] \right\}^{\frac{1}{2}}$$

And:

$$g = \frac{P_1}{P_I}$$

$$W_f = \alpha_1 \, g^{\frac{k+1}{2k}} \quad \text{lb/sec}$$

4. From the ideal gas law -

$$P_1 V_1 = W(t) \, R T_1$$

Where

$P_1 = \text{lb/in}^2$ (absolute)
$V_1 = \text{in}^3$
$R = \text{ft-lb/lb-°R}$

Then:

$$W(t) = \frac{P_1 V_1}{12R} \left[\frac{1}{T_I g^{\frac{k-1}{k}}} \right]$$

$$W(t) = \frac{g \, V_1}{12(530)} \left(\frac{P_I}{R}\right) \left[\frac{1}{g^{\frac{k-1}{k}}} \right]$$

Let -

$$\alpha_2 = \frac{P_I}{12(530)R}$$

Then -

$$W(t) = \alpha_2 V_1 \, g^{\frac{1}{k}}$$

(mass of gas left in small reservoir at any time)

Also -

$$W(t) = \frac{P_I \, V_I}{12R \, T_I} - \int_o^t W_f \, dt$$

Let -

$$\alpha_3 = \frac{P_I \, V_I}{12(530)R}$$

$$W(t) = \alpha_3 - \int_o^t W_f \, dt$$

5. Considering the piston displacement (S)

$$V_1 = (S_I - S) \, A$$

$$\frac{d^2S}{dt^2} = - \frac{1}{A} \frac{d^2V_1}{dt^2}$$

The damping force (F_3) is proportional to the piston velocity

Let Q = Constant of proportionality

Then -

$$F_3 = Q \frac{ds}{dt} = - \frac{Q}{A} \frac{d^{V}1}{dt}$$

$$\frac{d^{2V}1}{dt^2} = - \frac{A}{M} \left[A(P_3 - P_1) - F_1 - F_2 + \frac{Q}{M} \frac{d^{V}1}{dt} \right]$$

$$\frac{d^{2V}1}{dt^2} = - \frac{A^2 P_3}{M} + \frac{A^2 P_I g}{M} + \frac{A}{M} \left[F_1 + F_2 \right] - \frac{Q}{M} \frac{dV_1}{dt}$$

When the piston advances, V_3 increases -

$$V_3 = V_{3I} + \left(V_I - V_1 \right)$$

$$P_3 = P_I \left[\frac{V_{3I}}{V_3} \right]^k$$

$$P_3 = P_I \left[\frac{V_{3I}}{V_{3I} + V_I - V_1} \right]^k$$

$$P_3 = P_I V_{3I}^{\ k} \left(V_{3I} + V_I - V_1 \right)^{-k}$$

Let:

$$\alpha_4 = \frac{A^2 \ P_I \ V_{3I}^{\ k}}{M}$$

$$\alpha_5 = \frac{A^2 \ P_I}{M}$$

Then -

$$\frac{d^{2V}1}{dt^2} = \alpha_5 \ g - \alpha_4 \ (V_{3I} + V_I - V_1)^{-k} + \frac{A}{M} \left[F_1 + F_2 \right] - \frac{Q}{M} \frac{d^{V}1}{dt}$$

6. Equating expressions for w(t) -

$$a_2 V_1 g^{\frac{1}{k}} = a_3 - \int_o^t W_f \, dt$$

Differentiating with respect to time -

$$a_2 g \frac{dV_1}{dt} + \frac{a_2 V_1 g}{k}^{\frac{1-k}{k}} \frac{dg}{dt} = - W_f = - a_1 g^{\frac{k+1}{2k}}$$

Rearranging -

$$\frac{dg}{dt} = \left[- \frac{a_1}{a_2} Kg^{\frac{3k-1}{2k}} - Kg \frac{dV_1}{dt} \right] \frac{1}{V_1}$$

Let -

$$a_6 = - \frac{a_1}{a_2} K$$

$$a_7 = \frac{3k-1}{2k}$$

$$\frac{dg}{dt} = \left[a_6 g^{a_7} - Kg \frac{dV_1}{dt} \right] \frac{1}{V_1}$$

Equations to be solved:

A. $$\frac{d^2V_1}{dt^2} = a_5 g - a_4 (V_{3I} + V_I - V_1)^{-k} + \frac{A}{M} (P_1 + P_2) - \frac{Q}{M} \frac{dV_1}{dt} \quad in^3/sec^2$$

B. $$\frac{dg}{dt} = \left[a_6 g^{a_7} - Kg \frac{dV_1}{dt} \right] \frac{1}{V_1}$$

By reducing equation A into two first order differential equations the three resulting simultaneous equations (A1, A2, B) may be solved numerically by a Runge-Kutta method.

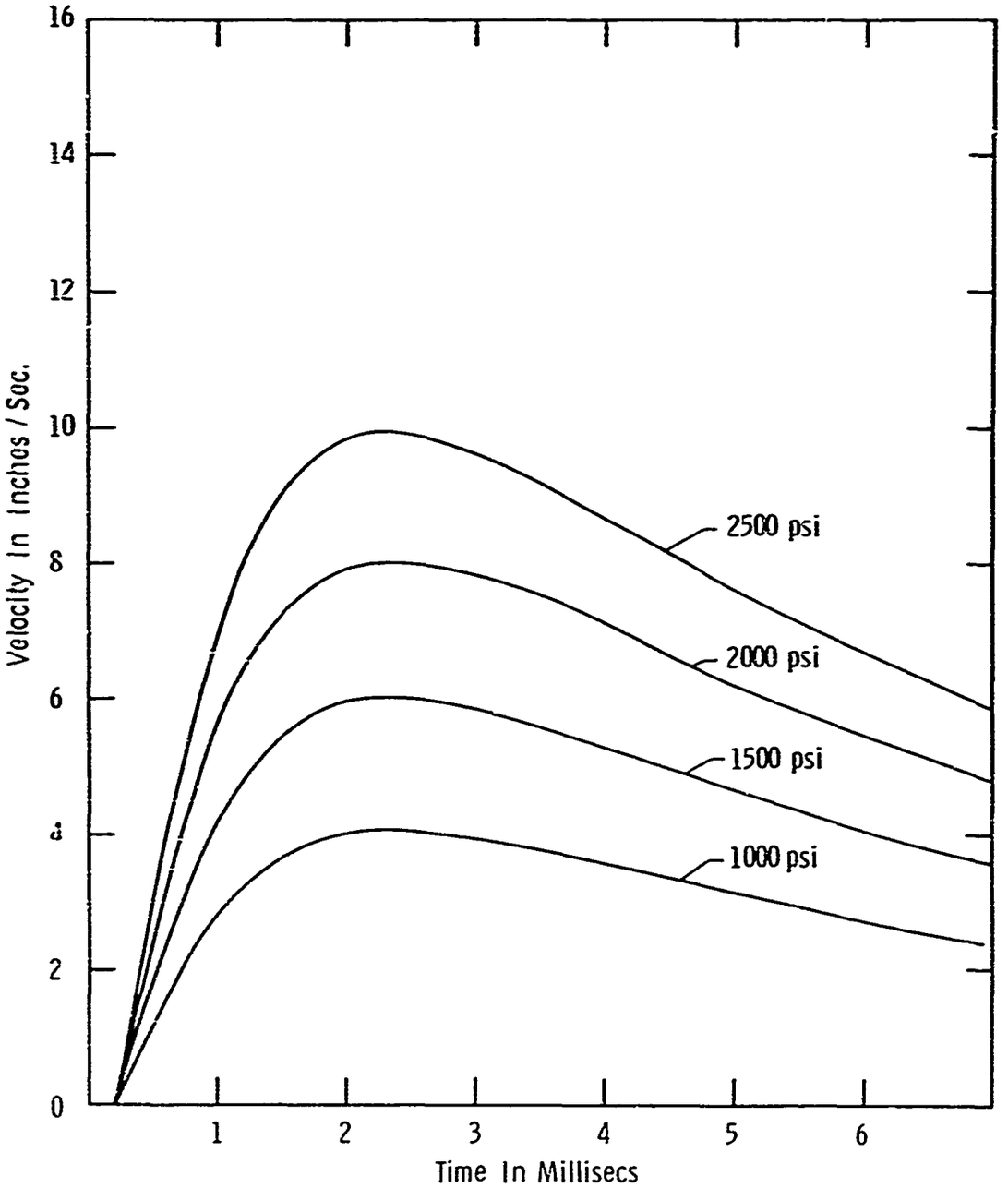

Figure B-2 Example of the Effect of Initial Reservoir Pressure on Piston Velocity

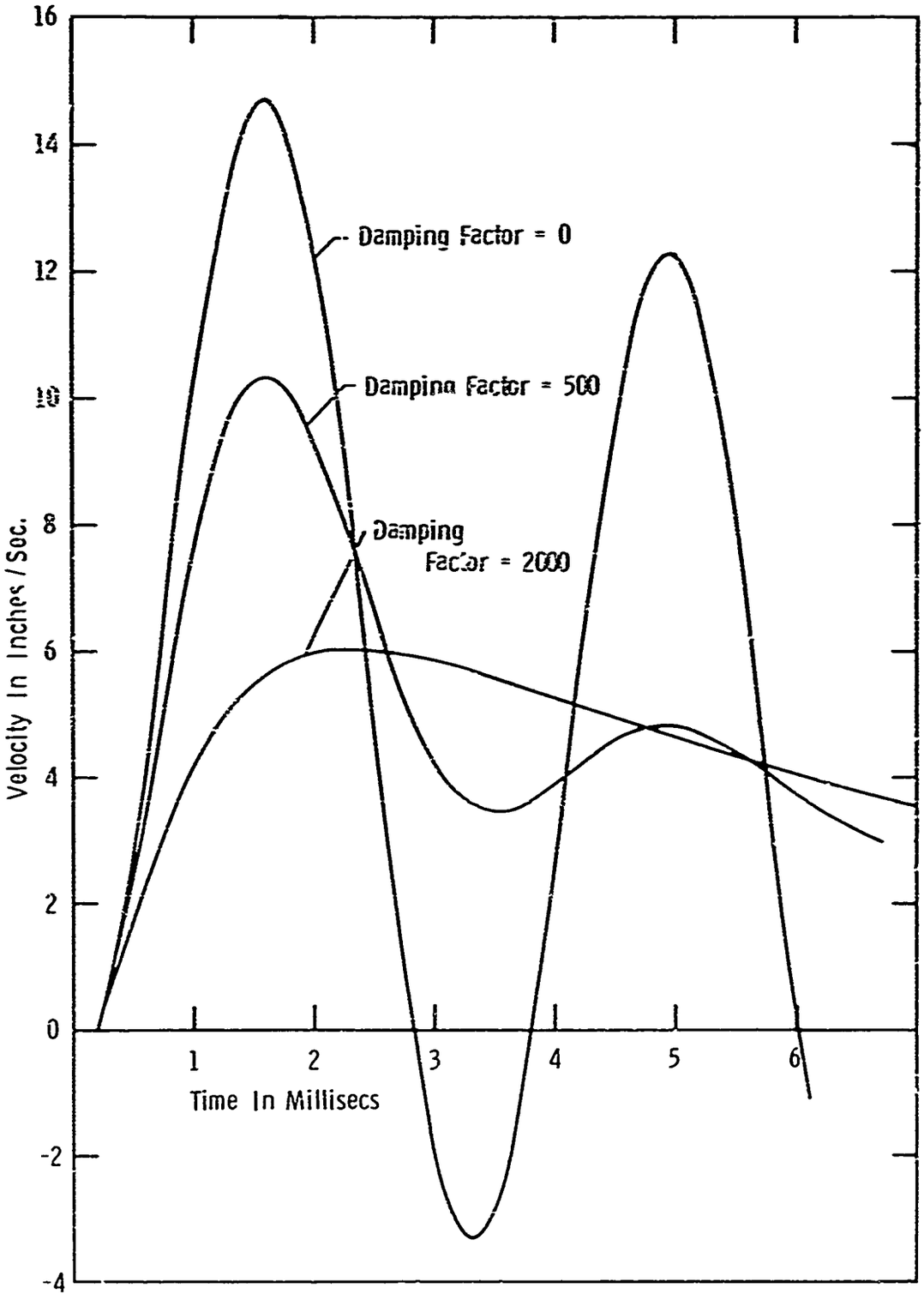

Figure B-3 Example of the Effect of Damping on Piston Velocity

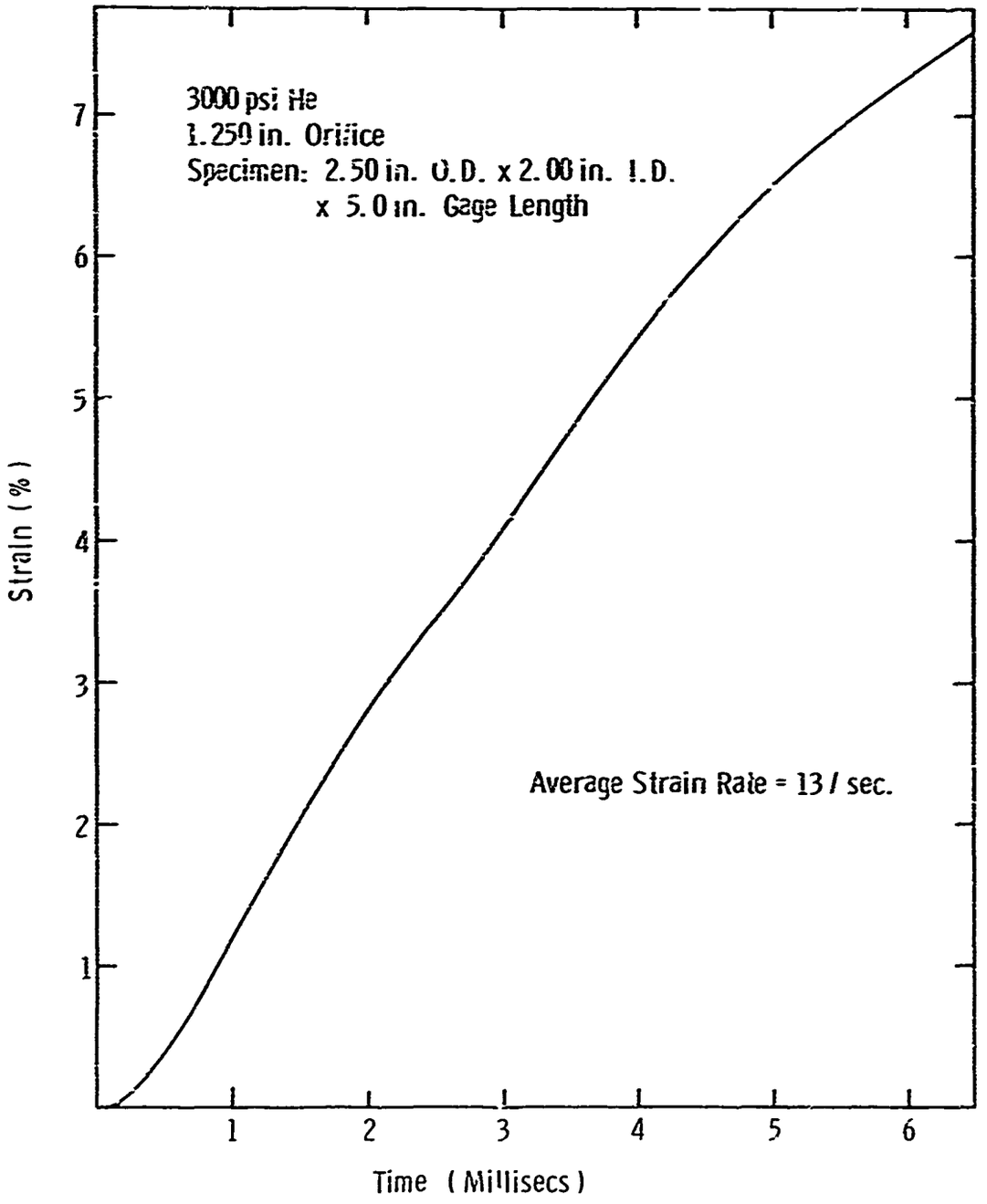

Figure B-4 Predicted Axial Strain on a Quartz Phenolic Tube

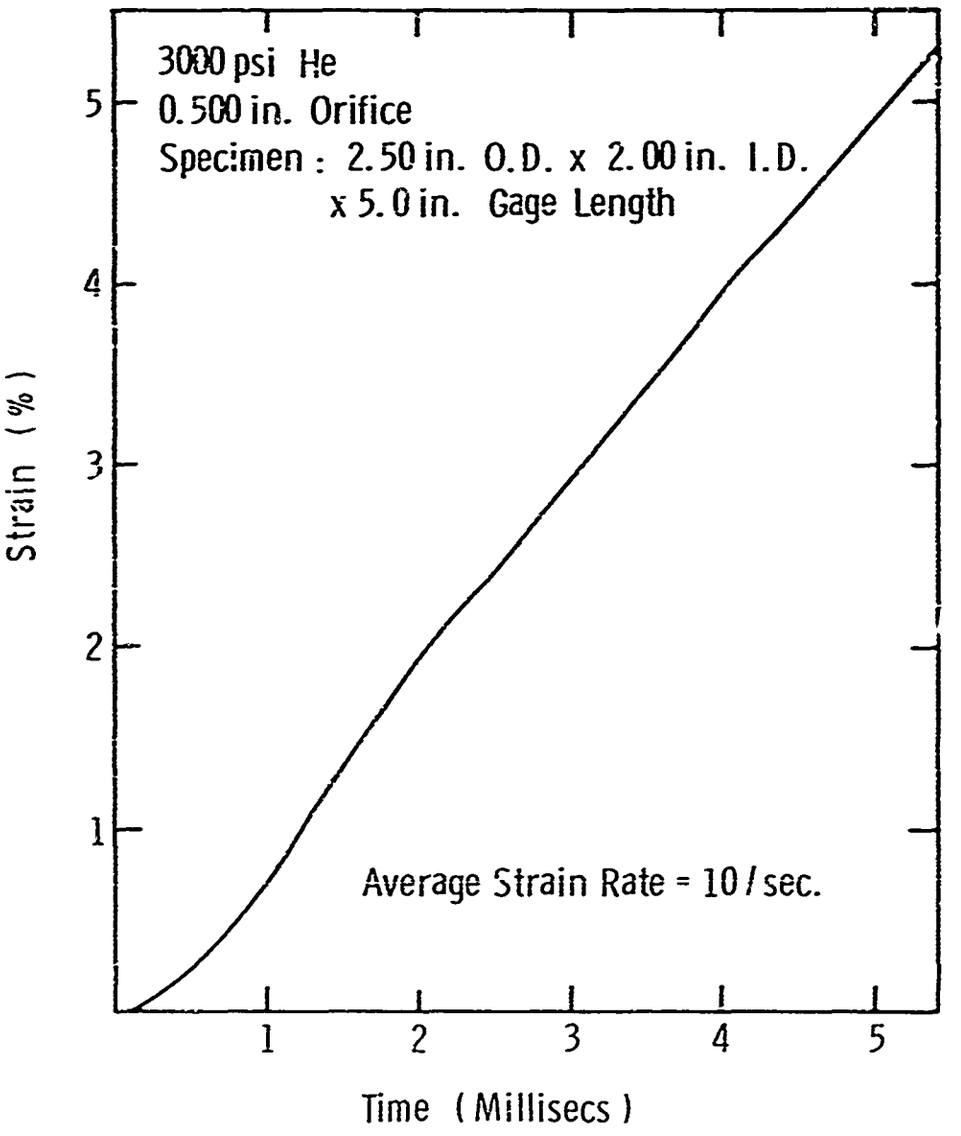

Figure B-5 Predicted Circumferential Strain on a Quartz Phenolic Tube

APPENDIX C

DETAILS OF FRAME PRELOAD

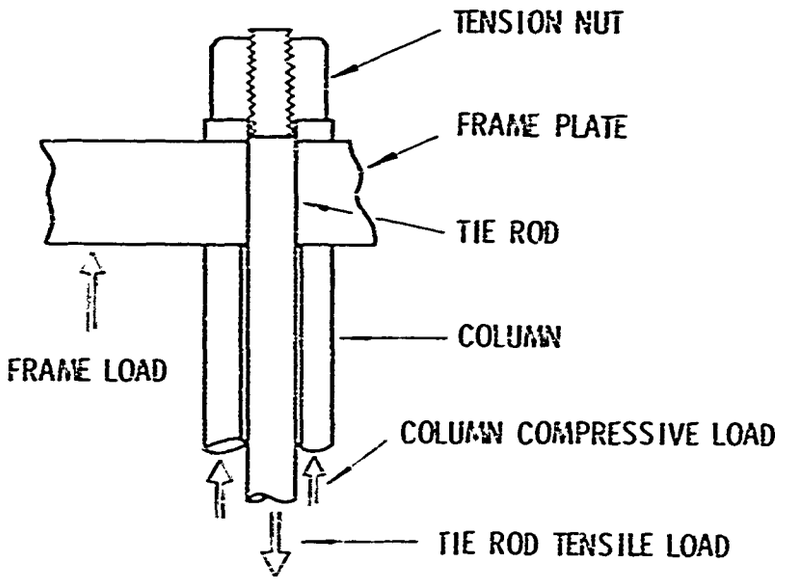

Figure C-1 Force System for Frame Preload

Definitions:

P	= Preload	(lb)
C	= Column Compressive Load	(lb)
T	= Tie Rod Tensile Load	(lb)
A_c	= Column Area	(in^2)
A_t	= Tie Rod Area	(in^2)
L_c	= Column Length	(in)
L_t	= Tie Rod Length	(in)
F	= Frame Load	(lb)
E	= Modulus of Elasticity	(lb/in^2)

Assuming elastic behavior, the ratio of force to deflection for the tie rod and column are:

$$\frac{C}{\Delta_c} = E\left[\frac{A_c}{L_c}\right]$$

$$\frac{T}{\Delta_t} = E\left[\frac{A_t}{L_t}\right]$$

Let Q = Equilibrum load on the tie rod and column after shrinking (LBS)

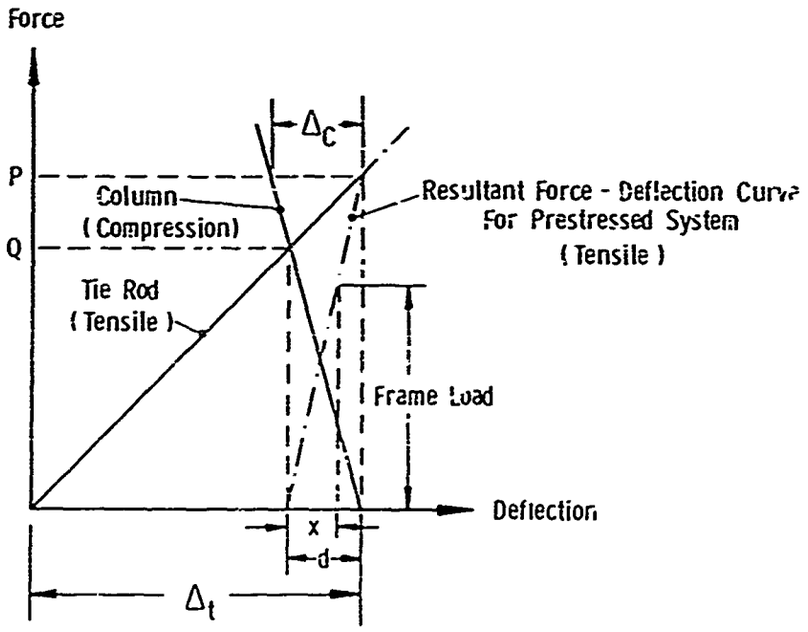

Figure C-2 Force - Deflection Behavior of Tie Rods

If the tie rod is loaded in tension to a load "P", the rod stretches a distance "Δ_t". If the column is loaded by the same force "P", it compresses a distance "Δ_c". Figure C-2 shows the relationship of these deflections. For shrunk tie rod construction the rod is stretched a distance "Δ_t", the

clamp nut is run down to contact the frame plate, and the rod is relaxed. As the rod relaxes, its length decreases. At the same time, the column starts to deflect in compression. As shown in the figure, when the rod is loaded with a force "P", the column load is zero. As the rod load decreases to load "Q", the column load rises to load "Q" and the system is in equilibrium.

The decrease in rod deflection and increase in column deflection is equal to "d". If a frame load "F" is now applied to the prestressed system, such as to increase the rod tension, the rod will deflect a distance "x". When the frame load "F" equals the preload "P", the column no longer is loaded and any increase in frame load is carried by the tie rods. The allowable frame deflection is then "d". In this machine the frame load will not exceed 80% of the preload.

To calculate d:

$$\frac{Q}{d} = \frac{P}{\Delta_c}$$

$$\frac{Q}{\Delta_t - d} = \frac{P}{\Delta_t}$$

$$Q = \frac{Pd}{\Delta_c} = \frac{P(\Delta_t - d)}{\Delta_t}$$

$$d = \frac{P\Delta_t\Delta_c}{P\Delta_t + P\Delta c} = \frac{\Delta_t\Delta_c}{\Delta_t + \Delta_c}$$

But:

$$\Delta_t = \frac{PL_t}{EA_t} \qquad \Delta_c = \frac{PL_c}{EA_c}$$

$$d = \frac{P}{E}\left[\frac{A_c}{L_c} + \frac{A_t}{L_t}\right]^{-1}$$

In particular, if $L_c = L_t = L$

$$d = \frac{P}{E}\left[\frac{L}{A_t + A_c}\right]$$

$$\frac{X}{F} = \frac{d}{P}$$

$$X = \frac{F}{E}\left[\frac{L}{A_t + A_c}\right]$$

If the frame load acts to increase the column load in contradistinction to the previous case, the limiting deflection is dependent on the column allowable stress. In the figure, the deflection will be to the left of the tie rod-column intersection point.

Thus it can be shown that a decrease in deflection is obtained with a prestressed construction whether the load to be resisted acts to shorten or lengthen the column.

UNCLASSIFIED
Security Classification

DOCUMENT CONTROL DATA - R&D

(Security classification of title, body of abstract and indexing annotation must be entered when the overall report is classified)

1 ORIGINATING ACTIVITY (Corporate author) Manufacturing Development, General Motors Corporation, GM Technical Center, Warren, Michigan 48090

2a REPORT SECURITY CLASSIFICATION: UNCLASSIFIED

2b GROUP

3 REPORT TITLE: FINAL REPORT MATERIAL RESPONSE STUDIES (MARS I), Vol III: Development of Multiaxial Stress High Strain Rate Techniques.

4 DESCRIPTIVE NOTES (Type of report and inclusive dates)
Final Report (in seven volumes)

5 AUTHOR(S) (Last name, first name, initial)
Green, S. J., Leasia, J. D, Perkins, R. D., Maiden, C. J.

6 REPORT DATE	7a TOTAL NO OF PAGES	7b NO OF REFS
January, 1968	60	47

8a CONTRACT OR GRANT NO: F04694-67-C-0033
b PROJECT NO
c
d

9a ORIGINATOR'S REPORT NUMBER(S): (14) MSL-68-8-Vol 3

9b OTHER REPORT NO(S) (Any other numbers that may be assigned this report): (15) SAMSO TR-68-71-Vol 3

10 AVAILABILITY LIMITATION NOTICES
This document may be further distributed by any holder only with specific prior approval of Space and Missile Systems Organization [redacted] Air Force Base, California [redacted].

11 SUPPLEMENTARY NOTES

12 SPONSORING MILITARY ACTIVITY: Space & Missiles Systems Organization, Air Force Systems Command, Norton Air Force Base, California 92409

13 ABSTRACT

Results reported ~~here~~ are on the development of techniques to determine material yield and/or fracture under multiaxial stress loadings at strain rates to (14) 10^2/second. An evaluation of various methods of biaxial and triaxial loading was made in order to determine a suitable method of testing both structural and ablator materials. Hence, the loading method and tubular specimen configuration are for nonhomogeneous, nonisotropic, brittle materials as well as more conventional ductile metals. A Biaxial Strain-Rate [redacted]chine has been built and some preliminary tests conducted. Details of the design and instrumentation are presented as well as preliminary data on an aluminum alloy.

DD FORM 1 JAN 64 1473

UNCLASSIFIED
Security Classification

KEY WORDS	LINK A		LINK B		LINK C	
	ROLE	WT	ROLE	WT	ROLE	WT
Multiaxial Composite Metals Strain-Rate Machine Design						

INSTRUCTIONS

1. ORIGINATING ACTIVITY: Enter the name and address of the contractor, subcontractor, grantee, Department of Defense activity or other organization *(corporate author)* issuing the report.

2a. REPORT SECURITY CLASSIFICATION: Enter the overall security classification of the report. Indicate whether "Restricted Data" is included. Marking is to be in accordance with appropriate security regulations.

2b. GROUP: Automatic downgrading is specified in DoD Directive 5200.10 and Armed Forces Industrial Manual. Enter the group number. Also, when applicable, show that optional markings have been used for Group 3 and Group 4 as authorized.

3. REPORT TITLE: Enter the complete report title in all capital letters. Titles in all cases should be unclassified. If a meaningful title cannot be selected without classification, show title classification in all capitals in parenthesis immediately following the title.

4. DESCRIPTIVE NOTES: If appropriate, enter the type of report, e.g., interim, progress, summary, annual, or final. Give the inclusive dates when a specific reporting period is covered.

5. AUTHOR(S): Enter the name(s) of author(s) as shown on or in the report. Enter last name, first name, middle initial. If military, show rank and branch of service. The name of the principal author is an absolute minimum requirement.

6. REPORT DATE: Enter the date of the report as day, month, year, or month, year. If more than one date appears on the report, use date of publication.

7a. TOTAL NUMBER OF PAGES: The total page count should follow normal pagination procedures, i.e., enter the number of pages containing information.

7b. NUMBER OF REFERENCES: Enter the total number of references cited in the report.

8a. CONTRACT OR GRANT NUMBER: If appropriate, enter the applicable number of the contract or grant under which the report was written.

8b, 8c, & 8d. PROJECT NUMBER: Enter the appropriate military department identification, such as project number, subproject number, system numbers, task number, etc.

9a. ORIGINATOR'S REPORT NUMBER(S): Enter the official report number by which the document will be identified and controlled by the originating activity. This number must be unique to this report.

9b. OTHER REPORT NUMBER(S): If the report has been assigned any other report numbers *(either by the originator or by the sponsor)*, also enter this number(s).

10. AVAILABILITY/LIMITATION NOTICES: Enter any limitations on further dissemination of the report, other than those imposed by security classification, using standard statements such as:

(1) "Qualified requesters may obtain copies of this report from DDC."

(2) "Foreign announcement and dissemination of this report by DDC is not authorized."

(3) "U. S. Government agencies may obtain copies of this report directly from DDC. Other qualified DDC users shall request through _____."

(4) "U. S. military agencies may obtain copies of this report directly from DDC. Other qualified users shall request through _____."

(5) "All distribution of this report is controlled. Qualified DDC users shall request through _____."

If the report has been furnished to the Office of Technical Services, Department of Commerce, for sale to the public, indicate this fact and enter the price, if known.

11. SUPPLEMENTARY NOTES: Use for additional explanatory notes.

12. SPONSORING MILITARY ACTIVITY: Enter the name of the departmental project office or laboratory sponsoring *(paying for)* the research and development. Include address.

13. ABSTRACT: Enter an abstract giving a brief and factual summary of the document indicative of the report, even though it may also appear elsewhere in the body of the technical report. If additional space is required, a continuation sheet shall be attached.

It is highly desirable that the abstract of classified reports be unclassified. Each paragraph of the abstract shall end with an indication of the military security classification of the information in the paragraph, represented as *(TS)*, *(S)*, *(C)*, or *(U)*.

There is no limitation on the length of the abstract. However, the suggested length is from 150 to 225 words.

14. KEY WORDS: Key words are technically meaningful terms or short phrases that characterize a report and may be used as index entries for cataloging the report. Key words must be selected so that no security classification is required. Identifiers, such as equipment model designation, trade name, military project code name, geographic location, may be used as key words but will be followed by an indication of technical context. The assignment of links, rules, and weights is optional.